UPGRADING LOW-GRADE IRON ORE BY MAGNETIZING ROASTING USING SAWDUST

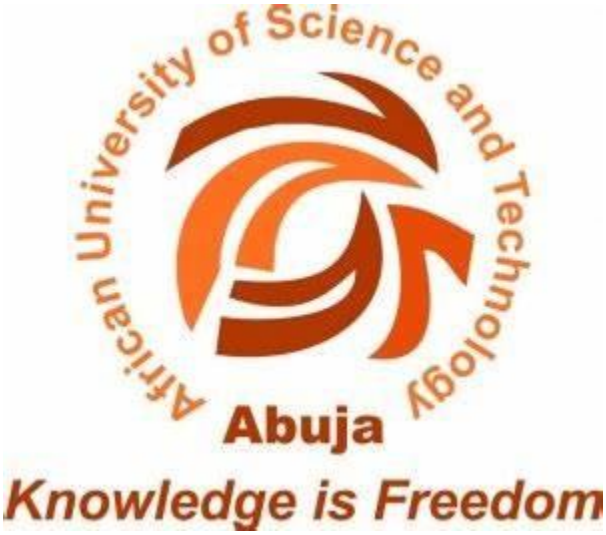

THIS THESIS IS SUBMITTED IN FULFILMENT OF THE REQUIREMENT

FOR MASTER OF SCIENCE DEGREE IN

(MINING AND MINERAL PROCESSING ENGINEERING)

MATERIALS SCIENCE AND ENGINEERING

BY

DARIUS GAYE WONYEN

SUPERVISED BY : PROFESSOR RICHARD AMANKWAH, VICE-CHANCELLOR
UNIVERSITY OF MINES AND TECHNOLOGY, UMaT GHANA

AT THE

AFRICAN UNIVERSITY OF SCIENCE AND TECHNOLOGY

ABUJA NIGERIA

March 16, 2021

UPGRADING LOW-GRADE IRON ORE BY MAGNETIZING ROASTING USING SAWDUST

By:

Darius Gaye Wonyen

A THESIS APPROVED BY THE MATERIALS SCIENCE AND ENGINEERING DEPARTMENT

Recommended: …….

Supervisor, Professor Richard Amankwah (11/03/2021)
Vice-Chancellor University of Mines and Technology
UMaT Ghana

……..
Head of Material Science and Engineering Department
Professor Azikiwe Peter Onwualu, FAS

Approved:……..……
Chief Academic Officer

Date: ……..

DEDICATION

This work is dedicated to the everlasting uncreated creator of the universe, Almighty God who has brought me this far. I also dedicate this work to my loving parents Mr. Moses B. Wonyen and Mrs. Esther N. Wonyen for their tireless and many countless supports that have made me come this far. I also dedicate this work to my fiancé Esther F. Bundoo and my son Michael D. Wonyen for their support, love, and courage throughout this time of academic challenges in the COVID era.

AFFIRMATION

I Darius Gaye Wonyen, do hereby declare that this thesis "**UPGRADING LOW-GRADE IRON ORE BY MAGNETIZING ROASTING USING SAWDUST**" is an original research undertaken by me at the department of Material Science and Engineering at the African University of Science and Technology (AUST) , Abuja Nigeria and that no part of this work has ever been submitted before for consideration towards another degree here and elsewhere and those works which are not my own have been appropriately and adequately referenced. I hereby submit this thesis for award of Master of Science degree in Mining and Mineral Processing Engineering (Material Science and Engineering) .

Darius Gaye Wonyen (ID: 40730)

Signature:…… | Date: 16th March 2021

ACKNOWLEDGEMENT

I am forever grateful to God Almighty for the success of this master's program. I acknowledge the support of my family. I am also thankful to my supervisor Professor Richard Amankwah, Vice-Chancellor University of Mines and Technology, UMaT, Ghana, for accepting me as a master's student and for guiding and supporting me throughout this research. I am also grateful to Professor Peter A. Onwualu, HOD, and the entire Materials Science and Engineering Department at AUST for their support. My immense gratitude to the Liberian Ambassador, Professor Dr. Al-Haslam Conteh for his instrumentality played and concern showed in my academic sojourn during my studies at AUST.

Most importantly, I owe a great due of thanks to the Arcelor Mittal family, Dr. Mark Van Dogen HR Global AM Mining, Mr. Lowe Scott CEO AML, Mr. Johannes Heytehch COO AML Liberia, and Ms. Rose Kingston HR AM Liberia for the educational subsidy provided in facilitating my graduate education.

ABSTRACT

Low-grade iron ore sample was collected from Gangra mines in Nimba Liberia. The ore was subjected to XRD and XRF analysis and was found to contain 63.1% Fe_2O_3, 25.4% SiO_2, 9.1% Al_2O_3, and 2.4% LOI. 561.5 g . 1684.5g raw ore was crushed, ground, screened to 2 mm particle size below and chosen for the study. 561.5g of this portion was subjected to dry magnetic separation and 50 g magnetic fraction was obtained and the remaining 1123.3g was divided in to two even portions and subjected each to three separate rounds of reduction roasting for 30 and 50 minutes and 61.4% and 65.9% of magnetic fractions were obtained, respectively. The mineral phase transformation of hematite to magnetite and other induced mineralogical properties due to reduction roasting were investigated using, energy dispersive spectroscopic EDX, scanning electron microscope SEM x-ray diffraction (XRD) and x-ray fluoresce (XRF) techniques. The effects of reduction variables such as time (30-50 mins), temperature (750-950^oC), and the reductant dosage were investigated as parameters that influenced the process. Carbon was obtained from carbonization of sawdust and was characterized and used as reductant. The results showed that the iron content in the magnetic fraction can be increased from 63.1% to 86.3% with parameters as follows: 950^oC heating temperature, average roasting time of 40 minutes, crushing, grinding, and mixing time of 2 minutes, reductant dosage of 10 g carbon 565.1 g of sample, and magnetic field strength of 0.2 Tesla. Complete hematite phase transformation to magnetite was obtained at the preceding conditions. Phase transformation was studied as a function of different roasting parameters and magnetic susceptibility. The feasibility of industrial application of reduction roasting followed by magnetic separation applied to low grade iron ore separation involving waste processing of sawdust as source of carbon as reductant is included.

KEYWORDS: Iron ore, phase transformation, magnetic separation, gravity separation, beneficiation, roasting temperature, comminution, pyrometallurgy.

TABLE OF CONTENTS

LIST OF TABLES

LIST OF FIGURES

LIST OF ABBREVIATION AND TECHNICAL TERMS

AML	:	Arcelor Mittal Liberia
AM	:	Arcelor Mittal
AUST	:	African University of Science and Technology
Canga	:	rocks of ferruginous laterite that form from any iron-bearing rock
		((conglomerate containing iron-formation clasts and ferruginous cement) and laterite form mappable bodies underlying relict land surfaces on the flanks of Nimba Range)
DRI	:	Direct Reduced Iron
DSO	:	Direct Shipment Ore
EDS	:	Energy dispersive X-ray Spectroscopy
Low grade	:	Iron ore consisting of (+/-45% Fe)
LGS	:	Liberian Geological Survey
SEM	:	Scanning Electron Microscopy
USGS	:	United States Geological Survey
XRD	:	X-ray Diffraction
XRF	:	X-ray Florence

CHAPTER ONE
INTRODUCTION, PROBLEM STATEMENT AND OBJECTIVES

1.1. INTRODUCTION

Iron ore is the chief raw material used to produce steel and other alloys of diverse kinds. Besides the recycling of different materials to produce iron, mining has been, and is the principal industry that is leading the world's supply of iron. Iron is the cheapest and the most used of all metals in the world and as an element occurs in several host ores or rocks (Susrut, 2019). Most iron ore deposits around the world and in West Africa are related to the Banded Iron Formation (BIFs) (Gunna et al, 2015): about 80-90% of the world production and reserve. Sedimentary deposits include bedded, layered, stratiform, and banded. A synonym to these types is the itabirite, taconite, jaspilite etc. The other origins of iron deposits and their locations around the world are magmatic deposit (Kiruna, Sweden; El Volca, Mexico); Otolithic Iron – riverbed (Robe River, Australia; Lisakovsky, Kazakhstan); Beach and River Sands deposit- placers (Arizona); Carbonate –hosted (Erzbera, Austria; Buvac, Bosnia); and Skarn (Kentobe, Kazakhstan) . The economic grade of iron ore today ranges from 20 -64% Fe (Arcelor Mittal University, 2014) with very few deposits enjoying extremely high grade. The grade of iron ore can be classified as low grade (+/-45% Fe) and high grade (65%Fe).

In Nimba, a county in Liberia, Gangra and Tokadeh ranges have two categories of direct shipment ores (DSO-1 and DSO-2) followed by low grade ore and canga (Arcelor Mittal 2014, Eric Force 1983) . These ranges are heavily dominated by weakly metamorphosed- sedimentary structures of rocks (Eric Force 1983 , LGS 2014, USGS 2012). The Geological age range of iron formation in Liberia is dominated primarily by the occurrence of Precambrian rocks emanating

from the Archean (Liberian) age in the west of the country and to the east of the country by the Proterozoic (Eburnean) age (Gunna et al, 2015). These formations are thought to have occurred in the 2.5-2.0 billion years in the middle of the Precambrian, hence, Liberia in comparison to other countries in the west African craton has suitable geology for prediction of a range of metallic and industrial minerals of which iron ore is dominant (Gunna et al, 2015) . There are about 5400 minerals identified on our planet but of these, over 1260 have been found to bear iron in their crystal structure (Arcelor Mittal,2014). Out of this total, 56.4% (771 minerals) have over 10% Fe in their chemical composition; 15% (187 minerals) have more than 30% Fe. However, only 4 of these iron -bearing minerals (Hematite, Magnetite, Goethite and Siderite- three oxides and one carbonate) are effectively used to supply the world's steel production (Arcelor Mittal). Though rarely encountered in iron ores, Maghemite (Υ- Fe_2O_3) may be included in this list.

Liberia has a huge deposit of iron ore mainly of the BIF metamorphosed- sedimentary deposit with high grade direct shipment ore (DSO) of 65% Fe that is currently being mined by the largest Steel Company in the world (Arcelor Mittal University). Beside crushing and screening, the ore is not being concentrated in the country. The current operation is targeted at high grade DSO but low-grade iron ore and canga ore are currently not being sort after hence they are stockpiled waiting for suitable upgrading to meet market demand post DSO depletion.

In this research, reduction roasting followed by magnetic separation is conducted to improve the magnetic susceptibility of paramagnetic minerals to ferromagnetic minerals. The research sets out to investigate how roasting time, temperature, and reductant dosage effects constituent chemical composition, phase transformation and composition, particle size distribution, and magnetic susceptibility which in turn influence grade and recovery of iron concentrate. Low grade iron ore sample was obtained from Gangra, Nimba Liberia was crushed, grind and

screened. The raw ore was characterized by chemical element and chemical iron phase, XRD, SEM/ EDX and XRF and subjected to low intensity magnetic separation. Some fractions of the ore were then mixed with sawdust (carbonized) and roasted in a furnace. Following the roasting, the roasted ore was subjected to magnetic separation and the product were characterized by XRD analyses to determine the phase composition and transformation. The results of roasted and unroasted magnetic products were compared and following that, the feasibility of industrial application of reduction roasting magnetic separation as suitable upgradation method of low-grade iron ore from Liberia was discussed.

1.2. PROBLEM STATEMENT

Iron ore mining is currently ongoing in Liberia on an industrial scale with crushing and screening of direct shipment ore gradually drawing near to depletion. In the Gangra and Tokadeh mountains of Nimba county, low grade iron ore assaying between 45-55 % Fe, SiO_2 greater than 8% and Al_2O_3 below 1% along with Canga assaying > 55% Fe, SiO_2 < 3% and Al_2O_3 > 5% are currently being stockpiled pending upgrade to reach market demands. It is of no doubt that the high-grade iron ore resources are slowly being exhausted and so their supply to the steel plant is being sharply declined. Post DSO completion from the Gangra and Tokadeh mountains, it can be expected that soon, the ore supply scenario will be difficult because of commissioning several steel plants and sponge iron plants around the world. The optimum and most economical way to overcome this challenge is to utilize low-grade ores, fines, and slimes that have been stockpiled in Tokadeh and Gangra mines sites/dumps for several years. At post completion of DSO shipment, these remaining iron resources would be valuable choices to continue production hence they warrant suitable beneficiation mechanism to meet the required value they need for

supply to the market. This beneficiation will require liberation and concentration in Liberia which has not really occurred before and may improve national value addition and create jobs when these ores are concentrated locally. Several methods have been proposed by different authors (Mishra, et al 2007, Y. Sun et al. 2020, Xiaolong Zhang et al 2019) to beneficiate these low-grade iron ore but the literature remains silent on upgrading low grade iron ore from Liberia to meet market demand. With the rising price of iron ore, and the depletion of high-grade iron ore, post DSO depletion, the low-grade iron ore and canga resource will be potential resource to overcome the shortages. The current methods of low-grade iron ore treatment are ultrasonic treatment, reduction roasting, microwave treatment, segregation roasting and colloidal coating. The alumina content in these low-grade ore present a serious problem to their beneficiation as hydroxy minerals like goethite (massive, earthly and colloform) and limonite ultra-fine particle, poor liberation (-150 micrometer) present problem to their deposition. There is still work ongoing to propose optimum beneficiation strategy to concentrate these low-grade ore locally. Hence it is imperative to investigate new ways in which these resources can be upgraded locally to meet market demand and increase national gross product and employments. Usually there are several paramagnetic and ferromagnetic minerals in iron ore. To improve the amount of iron concentrate from magnetic separation of low-grade iron ore it is important to understand the following: constituent minerals and chemical element present, phase composition and transformation, particle distribution and mineral disseminations.

1.3. OBJECTIVE OF STUDY

The primarily objective of this research is to investigate the effect of reduce roasting on mineral phase composition and magnetic susceptibility of low-grade iron ore.

Therefore, the main research questions to answer in achieving the objective are the following:

a. How roasting temperature and roasting time affect the phase composition and magnetic susceptibility of roasted ore?
b. What is the theoretical amount of carbon dosage required to carry out the reduction of low-grade iron ore?
c. How do roasting parameters affect the grade and recovery of magnetic fraction of roasted products?

CHAPTER TWO

1.0 LITERATURE REVIEW

2.1. Geology of Nimba Iron Ore Deposit

The Republic of Liberia as shown in *figure 2.1* is a country located in west Africa and bounded by three countries and the Atlantic Ocean. Liberia's geology is influenced by the geology of the west African craton and the country is dominated by geologic structures tracing their routes (Gunna et al 2015). The country is underlain chiefly by Precambrian rocks of Archaean (Liberia) age in the west and the east by the Proterozoic (Eburnean) age (Gunna et al 2015). The land area of Liberia is approximately 111,000 km^2 with fifteen political division called counties and a

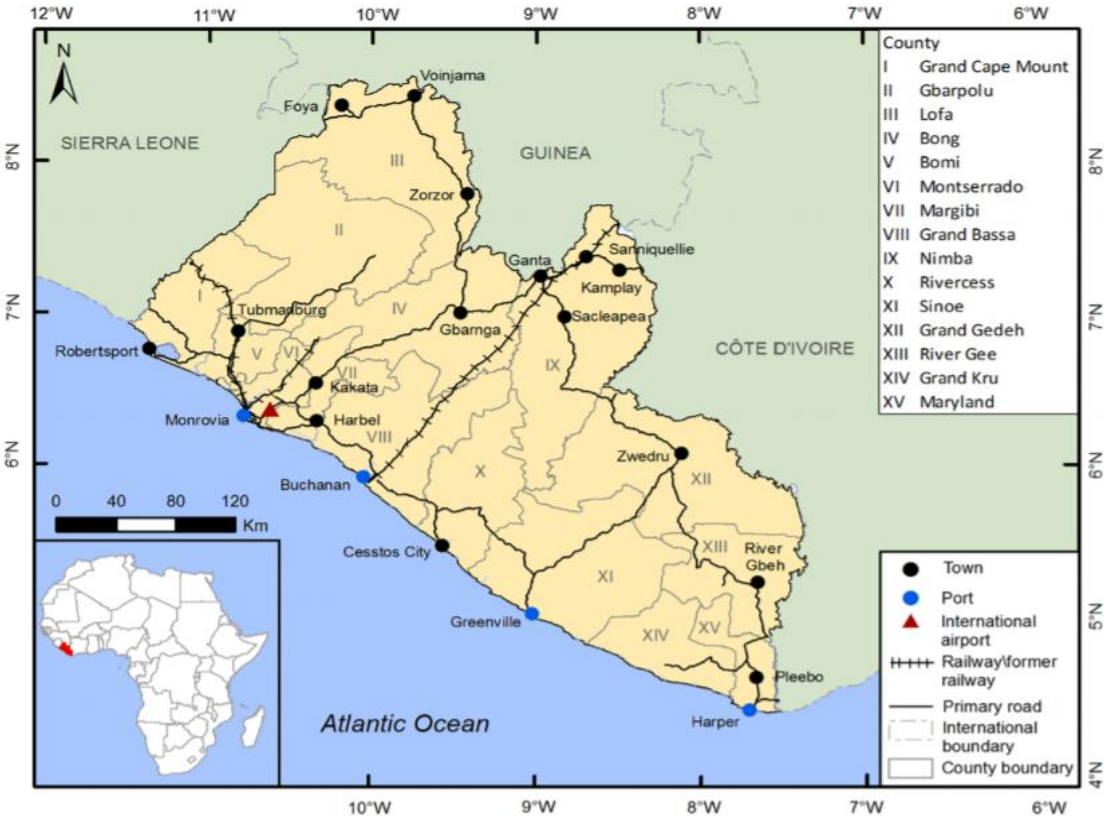

Figure 2.1. Location of major transport infrastructures of Liberia (*Gunn et al 2015)*

population of approximately 5.0 million people. The land mass is decorated with rolling plateaus, low mountains and some narrow flat coastal plain. Mount Wutivi in Lofa county is measured 1,400 m to be the highest elevation followed by the Nimba mountain measured 1,300 m in Liberia (Gunna et al 2015). Liberia's climate is typically tropical, hot, and humid at nearly all time with two seasons having rain and summer distributed equally over six months periods. The geology of the country like other locations in west Africa is favorable for occurrence of different metallic and industrial minerals such as iron ore, gold, diamonds, cupper and bauxite and barite as well as some rare earth minerals. Out of these, the country's mining industry from 1960s up to the beginning of the civil war in 1990s, had contributed more than 20% of the gross national product and employment more than 50,000 which accounts approximately 15% of the country's total work force (Gunna et al 2015). As shown in *figure 2.1* the major transportation route of iron ore is via a rain track that extend form Nimba County down to the port of Buchana. There is one international Airport in the country with a host of nonfunctioning local airports spread across the nations. Liberia has four major functioning ports with the Port of Buchanan experiencing the export of iron ore commodities being mined from the Nimba Mountain. Primary unpaved roads connect many counties with few major highways extending out of Monrovia to the hinterlands.

Iron ore mining in Liberia is continuing after the civil war with the Nimba range experiencing exploitation of direct shipment ore, low grade and canga. The geology of Nimba is part of the Proterozoic (Eburnean) age. Three tectonic terranes categorize the Precambrian rocks of Nimba (Eric Force 1983 , Gunna et al 2015, LGS 2014 , USGS 2012) . The first terrane is the called the Nimba block which is of the Nimba Supergroup supracrustal rocks and is dominated by isoclinal folds. The second terrane is the Gbedin-Kahnple block which is mainly dominated by folded granitic gneiss basement that is unconformably overlined by iron -formation and leucocratic

gneiss. The first two terrane are suitably juxtaposed in an indefinite way and re deformed, metamorphosed (locally to granulite) and intrusion from mafic rocks. The third terrane is dominated by diorite, supracrustal rocks, and mafic rocks which were later thrust over the first two. Juxtaposition in the terranes is independent of the records of folding and have been the

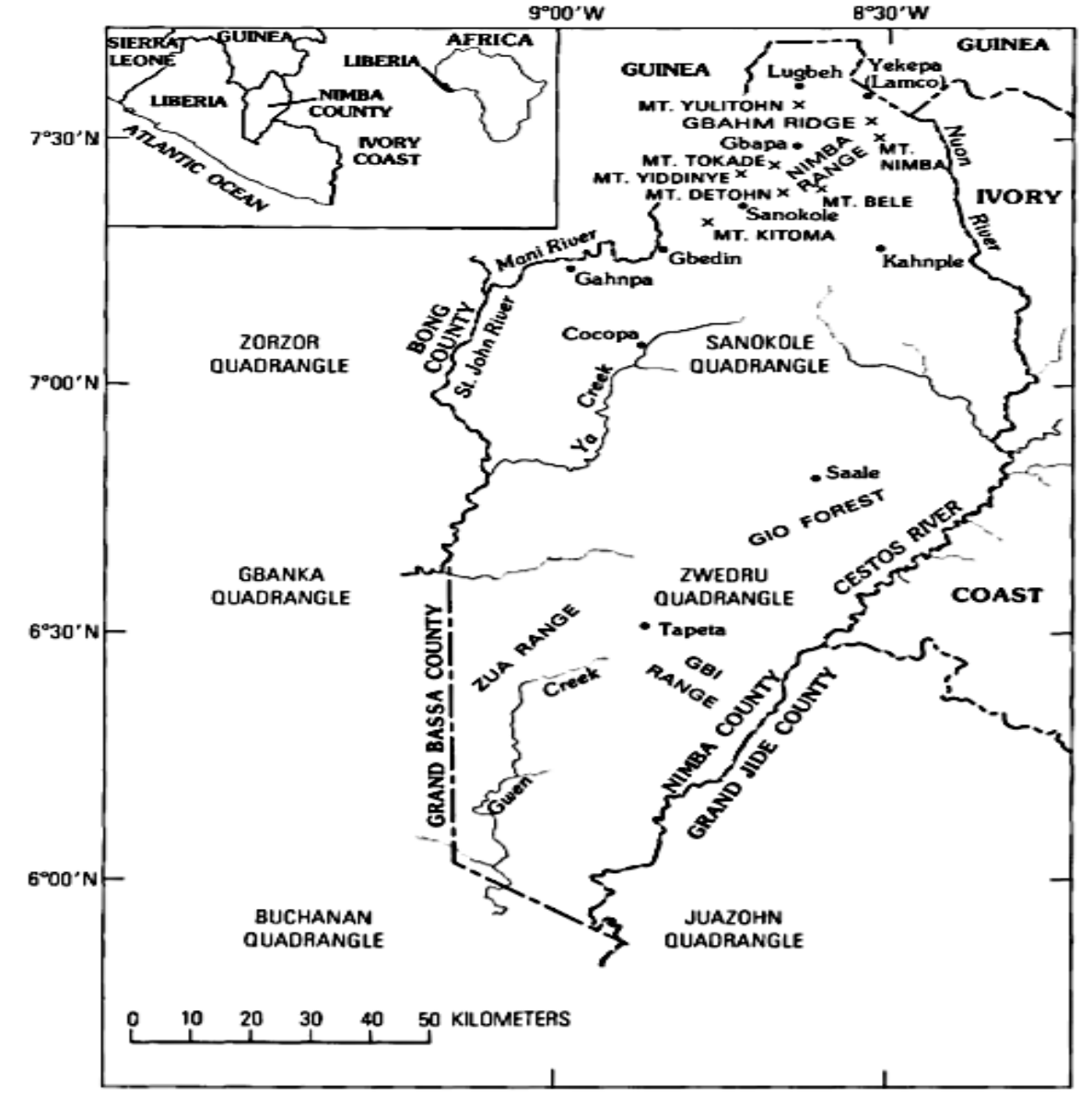

same thereafter and four-fold sets are identified (Eric Force, 1983).

Figure 2.2.a. Quadrangle boundaries and geographic localities of Nimba County

Nimba county has extension form 6^{o} to 8^{o} east with varying wet and dry seasons. Annual rainfall is truly little as 200em in the north and the temperatures are very normal in the highest parts of Nimba. There are several savannahs in higher attitude with rain forest dominating the entire

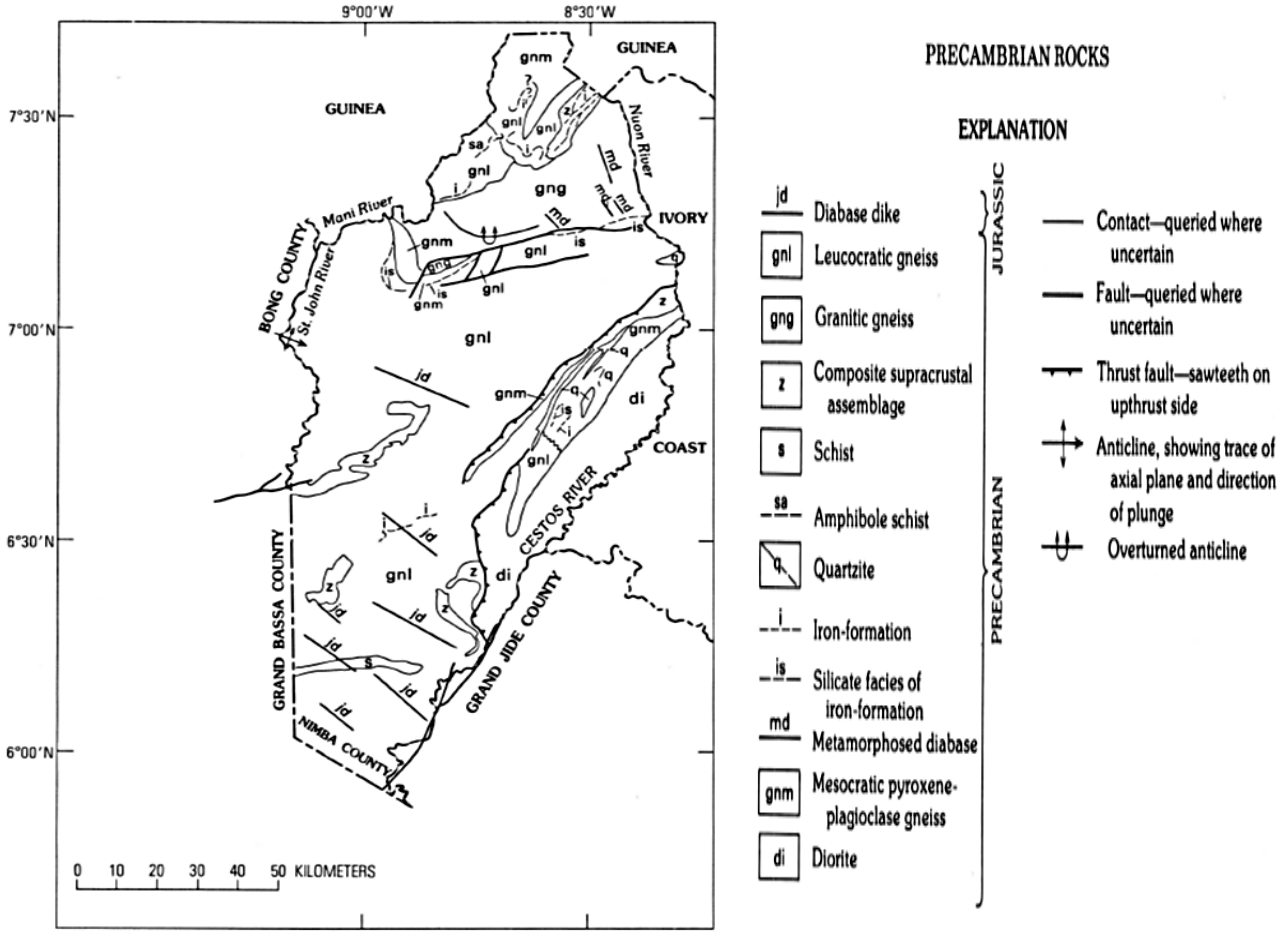

county.

[*units are described in text; Force, 1983 Geology of Nimba County, Liberia***]**

(Force, 1983 Geology of Nimba County, Liberia)

Figure 2.2.b. Quadrangle boundaries and geographic localities of Nimba County

2.1.1. Structure

Folds and faults are among several geologic structure found in Nimba county. Beside the folds that were mapped by Berge in 1968, there is little information of detail folds occurrence in Nimba even though there are reports of relative folds in the Sanokole Mt. Nimba area. In the northern half of Nimba county, four set of folds have been identified with two sets being juxtaposed and deformed to a younger set (Eric Force 1983 , LGS 2014 , USGS 2012). As shown in *figure 2.3*, F1 and F2 are from the past but they evidently formed individually, and their relative ages are undetermined. The first set of fold extends approximately 30 km southeast then northeast from Gbedin. It consisted of sizable eastward-closing refolded antiform. By traces in aerial photograph, hinges can be seen of how the foliation of granitic gneiss have occurred. Rocks of Mt. Kitoma are separated from this fold by a truncated fold of younger unconformity or fault. As shown in *figure 2.3,* the second fold is confined to the Nimba Supergroup and is seen in

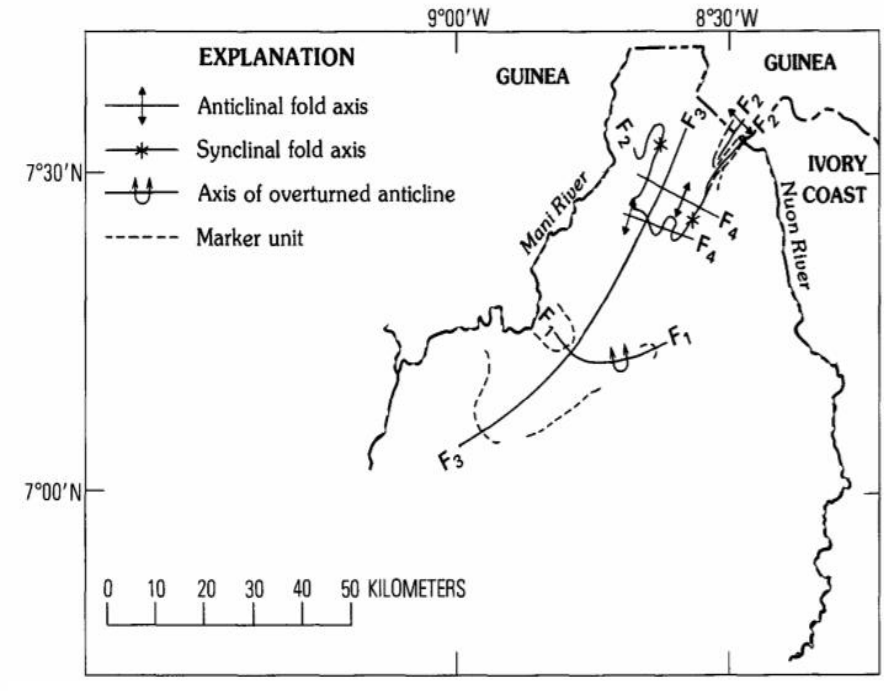

Figure 2.3 : Locations of folds of various ages in the Mt. Nimba-Sanokole

the Mt. Nimba – Gbahm Ridge area. The folds are closely isoclinal and has a plunge southwest and the plunge direction is further overturned south in the range. The itabirite at Mt. Bele, Mt. Tokadeh, and Mt. Yuliton can be correlated as syncline and they are like fold in the Mt. Nimba area (Eric Force, 1983). The third set of folds as shown in *figure 2.3* , has an axial plane which can be traced over 50km southwestward from the Nimba -range and it folds the other older folds of the Nimba Supergroup (F2), the fold granitic gneiss (F1) and iron-formation that covers granitic genesis . It consists of one huge open fold that closes at the southwest and around the Cocopa and Gbapa area, mesocratic pyroxene-plagioclase apparently intruded as sill along the hinges (Eric Force, 1983). The last fold (F4 in *figure 2.3*.) has northwest-trending free upward that impede the older ones in the Nimba Supergroup to create the recommended plunges seen in the Nimba Range and the dome-and basin pattern of iron formation to the west. As characteristic trend of the Pan- African (about 600m.y) deformation is parallel to this fold and this fold set can be thought of as a distal effect of deformation. There is conspicuous evidence of other folds in the iron-formation at south end of the Zua Range, in quartzite of the Gio Forest and iron-formation of the Gbi Range. This fold seems in aerial photograph to be refolded (Eric Force, 1983). In the east of Cocopa plantation, a sharp fracture separates the terrane into rhomb-shaped block and cut out across the band of iron formation in two places. Magnetic maps show that iron-formation is unceasing with extent. The principal fault in Nimba is a folded suture like fault, a thrust fault, northeast- trending shear zones and , and possibly conjugate set of fracture. As shown in *figure 2.3*., a suture like fault divides the terranes of F1 and F2 folding. Most noticeable fault in Nimba is the imbricate thrust in Gio Forest, which dips gently east and is characterized by thick mylonitic zones dominated by blastomylonites (Eric Force, 1983).

2.2. Mineralization of Nimba iron ore

2.2.1. Types of iron minerals

Iron formation is well suited in Nimba where the Nimba supergroup contains the oxide-facies of the Nimba itabirite which has been in mining operation before the civil war (Eric Force, 1983, A.G. Gunna et al 2015, LGS 2014 , USGS 2012) . At mount Tokadeh, Gangra, Yeuliton and Gbahm, simple oxide and carbonate -and silicate-bearing oxides faces are present because of different depositional circumstances. As indicated by the assemblages of actinolite-chlorite and orthopyroxene-garnet, metamorphic grade ranges from greenschist facies to pyroxene granulite are available (Eric Force, 1983, LGS 2014 , USGS 2012). At mount Kitoma which is of potential economic significance, oxide-facies magnetic iron-formation is present. Near Gahnpa and past Karnplay (*figure 2.2.a*), a silicate -facies iron formation(ies) extends more than 60 km as four separate sections. Banded iron has been formed because of mutable metamorphic situations.

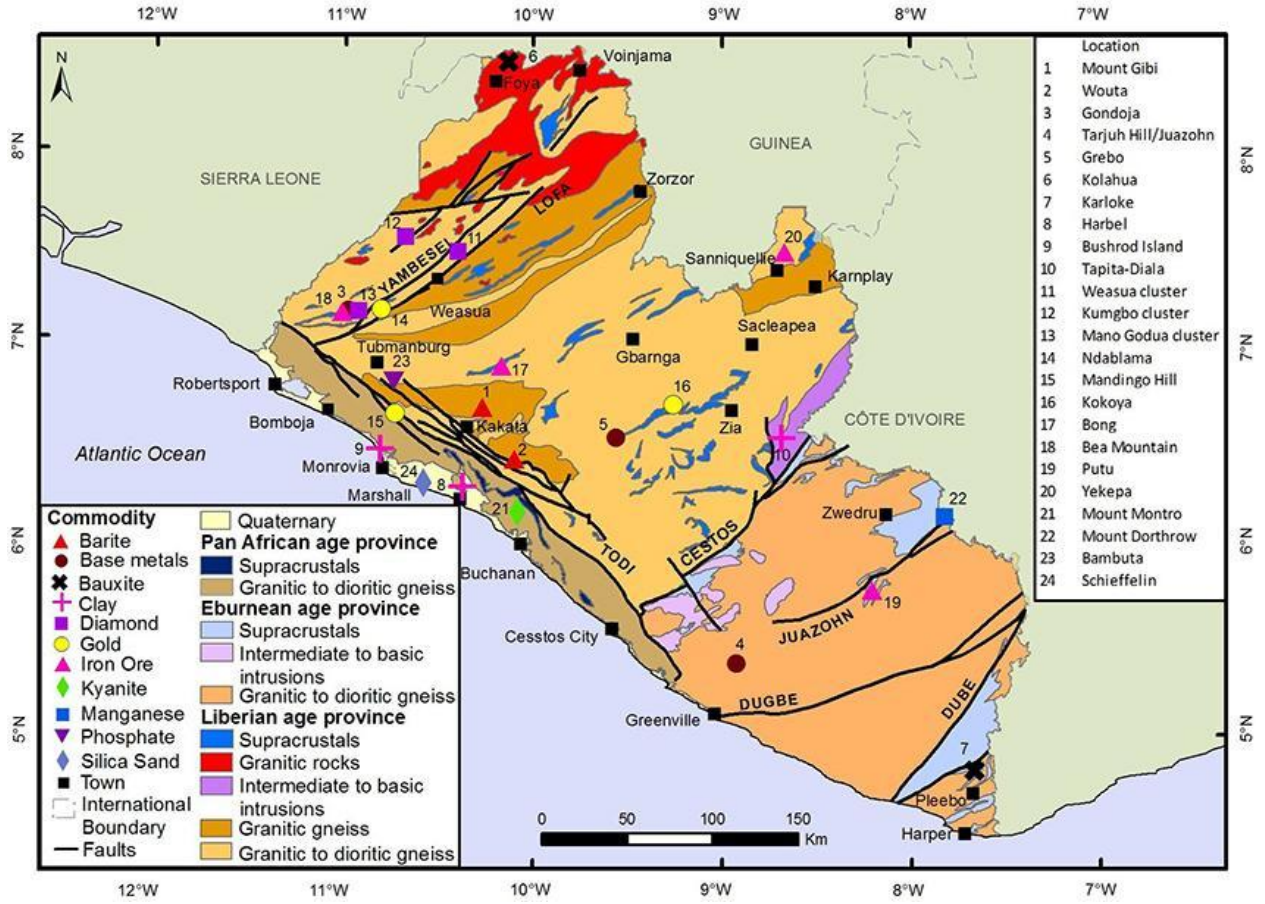

Figure 2.4 Mineral Potential Map of Liberia (*A.G. Gunn et al 2018*)

Before the civil war in the year 1980, iron ore mineral was mined in Mt. Nimba , Gbahm Ridge and Mt. Tokadeh by LAMCO at a production capacity of about 12 million tons per year (LGS 2014, Gunna et al 2015,) with high-grade ore (63-68% Fe) derived from itabirite (Oxide facies iron formation) of some metamorphic hydrothermal enrichment (hematitic "blue ore") and by deep weathering (goethite "brown ore",) (Berge, 1966).

Since its discovery in 1955, the reserve was estimated at 250 million tons (Berge, 1968) and the western reserve was estimated in 1978 at 535 million tons of having higher amount of magnetite and hematite's itabirite and are themselves low grade as shown in *Table 2.1*

Table 2.1. Chemical analyses of some Nimba iron-formation rocks

[values are in weight percent of oxides present; no entry indicates value not determined or less than 0.1. From

Oxides \ Sample No.	1	2	3	4	5	6	7	8	9
SiO_2	40.4	39.7	40.2	40.4	39.8	1.5	1.5	49.2	48.6
Al_2O_3	.4	.1	.3	.9	.3	.5	.8	3.7	6.4
Fe_2O_3	35.5	44.0	55.6	41.4	33.1	97.0	93.7	6.5	3.2
FeO	18.1	12.9	1.1	13.3	17.4			35.0	34.0
MgO	1.8	.6	.2	.1	1.8			3.3	4.1
CaO	1.8	.3	.7	1.2	2.3			.6	.7
Na_2O	.2								
K_2O	.2	.1		.2				.1	.1
P_2O_5	.2	.1	.2	.2	.2			.1	.1

[1]Average silicate-bearing itabirite, Mt. Tokade—Mt. Yulitohn.
[2]Average magnetic itabirite, Nimba.
[3]Average hematite itabirite, Nimba.
[4]Average silicate-bearing magnetic itabirite, Nimba.
[5]Average silicate-bearing itabirite, Gbahm Ridge.
[6]Average "blue" (hematite) ore.
[7]Average "brown" (goethite) ore.
[8]Orthopyroxene-garnet silicate facies, Cocopa area.
[9]Grunerite silicate facies, Kahnple area.

Berge, 1971- 1972, 1974; Force and others, 1971-197

Some oxide-facies and silicate -facies are present in the iron formation found at the Gio Forest (USGS). In the Gbi range, similar oxide-facies iron formation dominates a larger part with low grade ore presence and a few transverse of high-grade ore. In this region, some of the itabirite are rich in hematite other than magnetite of coarse grain (LGS 2014, Eric Force 1983). As shown in Table 2.2, the various valuable minerals found in iron core minerals are tabulated with their chemistry, grade, specific gravity, hardness, and magnetic nature.

Table 2.2. Value Iron bearing mineral in iron ore

Mineral	%Fe^{2+}	%Fe^{3+}	LOI %	Chemistry		Grade	SG	D_{Mohs}	Magnetism	Highlight
Magnetite	24.1	48.3	0.0	Fe_3O_4	$FeO.Fe_2O_3$	72%	5.1	6	Ferromag	Highly Magnetic
Hematite	0.0	70.0	0.0	$Fe2O_3$	Fe_2O_3	70%	5.3	6½	Paramag	Most important source
Goethite	0.0	62.9	10.1	FeOOH	$Fe_2O_3.H_2O$	63%	3.8	5	Paramag	Most impure (Al, Si,P)
Siderite	48.2	0.00	37.9	$FeCO_3$	$FeO.CO_2$	48%	4.0	3½	Diamag	Few applications

2.2.2. Gangue minerals

There are several unwanted minerals that exist in iron ore deposit. These minerals are usually referred to as gangue minerals and they often affect the choice of beneficiation of the iron ore. As shown in Table 2.3 several gangue minerals in iron ore deposit are tabulated along with their specific gravity, magnetic properties, and chemical compositions.

Table 2.3. Gangue Minerals in iron ore

Mineral	%SiO_2	%Al	%LOI	Chemistry		SG	Hardness Mohs	Magnetism	Highlights
Quartz	100.0	0.0	0.0	SiO_2	SiO_2	2.7	7	Diamag	Most common
Kaolinite	46.5	39.5	14.0	$Al_2Si_2O_5(OH)_4$	$Al_2O_3.2SiO_2.2H_2O$	2.6	2	Diamag	Source of silica & alumina
Gibbsite	0.0	65.4	34.6	$Al(OH)_3$	$Al_2O_3.3H_2O$	2.3	2½	Diamag	Major Al-bearing mineral (bauxite)
Apatite	0.0	0.0	1.8	$Ca_5(PO_4, CO_3)_3.(F,OH, Cl)$	$10CaO.3P_2O_5.H_2O$	3.2	5	Diamag	Major P source in Magnetic ores

2.3 Global iron ore production, price, and consumption

Iron ore is the chief raw material for the world steel making process (Arcelor Mittal, 2014). Since the early days of civilization, iron have been a key ingredient for civilization, weaponry, cooking utensil and many other useful applications. In this current age, the use for iron has expanded to many different applications due to good mechanical and thermal properties among others.

Iron is used in steel production as the primary ferrous metal and alloy and steel. Iron is used in fabricated products, machinery, structures, transportation equipment, space equipment, toy goods, and biomedical application as magnetite nanoparticles has emerged. These wide and increasing application of iron has made the extraction of this metal a great investment in the world and several large companies have established themselves as cartels. According to Iron Investing News, as of June 30th, 2020, Brazil, Australia, China, Russia, India, Ukraine , South Africa, Canada and United States were the top nine iron ore supplying countries in the world with China drawing the business routes of iron ore trade (Table 2.4). Vale's experienced collapse to their tailing dams at Corrego do Feijao mine in Brazil linked with the coronavirus pandemic in 2019. Due to this iron ore prices have risen reaching a five-year high-ranking of US $ 123.19 per ton ever since July 2019. Though the price of the base metal dropped as low as USD $80.36 per tonnes close to the end of last year, the corona virus in Brazil and the rest of the world.

Table 2.4. Top Iron Ore producing countries and companies.

Rank	Country	Usable Ore (Mt)	Iron Content (Mt)	Major producer
1.	Australia	930	580	BHP (NYSE:BHP,ASX:BHP,LSE:BHP)
2.	Brazil	480	260	Vale
3.	China	350	220	-
4.	India	210	130	NMDC
5.	Russia	99	59	-
6.	South Africa	77	49	Kumba Iron Ore (JSE:KIO)
7.	Ukraine	62	39	Black Iron (TSX:BKI,OTC Pink:BKIRF)
8.	Canada	54	33	Champion Iron (TSX:CIA,OTC Pink:CHPRF)
9.	United States	48	31	-

Source: Iron Investing news

the world has hindered iron ore production in that part of the world and caused higher price surge. According to reports from Zacks Investment Research released early June 2020, iron ore and gold are said to be the lone metals that have not experienced price falls as the result of the of the corona pandemic. Using most recent data provided by the US Geological Survey, nine countries can be said to be leading the iron ore production in the world currently. Table 2.4 shows the list of top iron ore producing countries and their major companies.

Despite being the third in the list, China is the world's top buyer of iron ore (USGS 2020).The usable domestic production of iron ore is not sufficient to supply for raw material for the stainless-steel demand since China is the largest producer of Stainless steel. As a result of this

China imports over 70% of the sea borne iron ore (Madhurima Das Zacks 2019). According- to

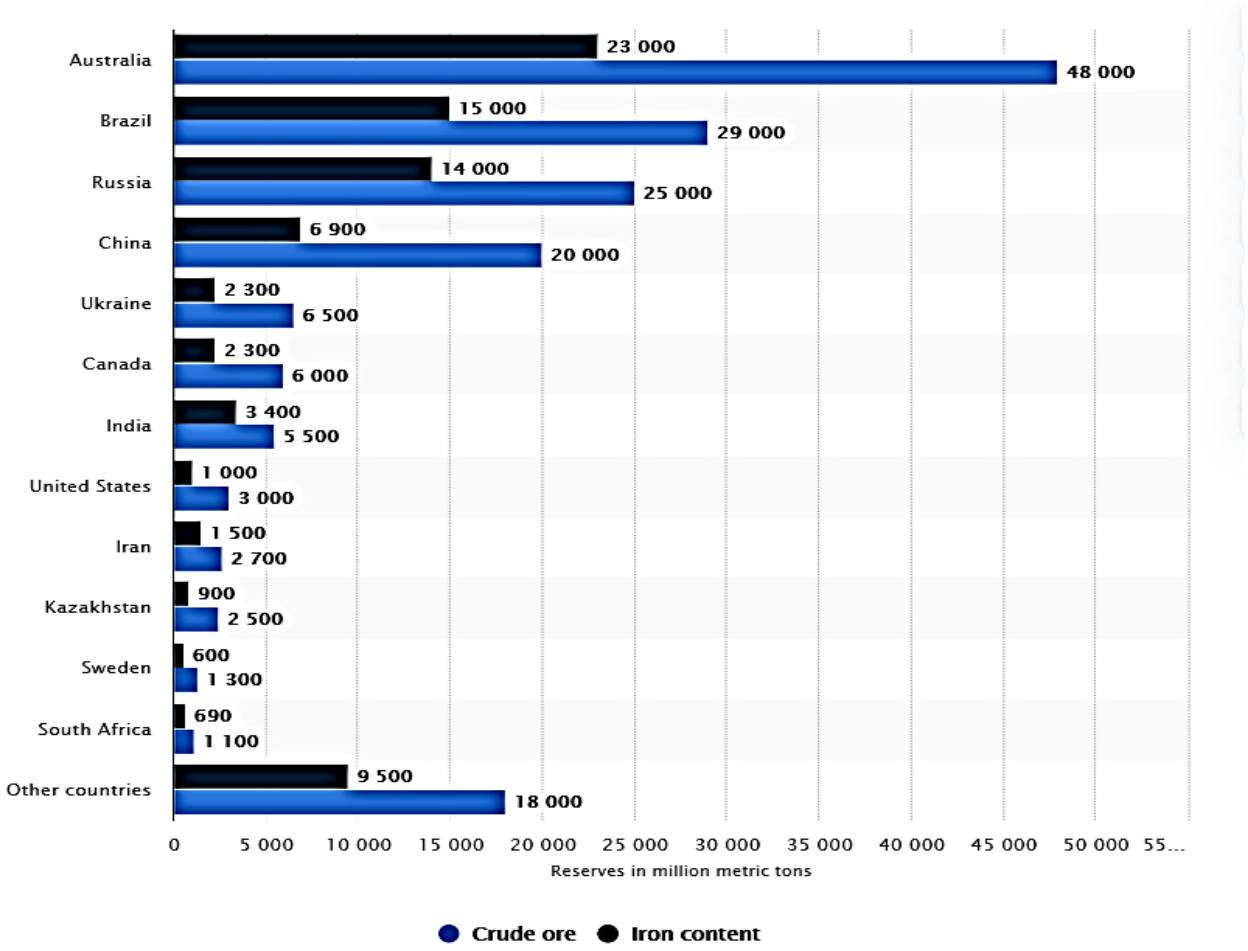

Figure 2.5. World reserves of iron ore as of 2019, by country (in million metric tons)

the same source, the economy of China is increasing and creating good demands form iron ore import following the coronavirus pandemic.

South Africa is the biggest supplier of iron ore in Africa with slight increase in production from 2018, its exploitable iron ore supply climbed from 74.3 Mt to 77 Mt in 2020 and iron content jumped from 47.2 to 49 million (Investing News).

Liberia ranks 27th on the expanded version of this list shown in Table 2.4 with 1930 thousand tonnes or usable ore production in 2017. Though not clearly shown in *figure 2.5*, Liberia contributes to the total number of other countries and in West Africa, Liberia has some of the largest reserves of iron ore with current production on going for DSO operation. In 2015, the United States Geological survey reported that Nimba holds approximately one billion tonnes of high-grade iron ore. In September 2019, Vancouver-based HPX acquired the deposit because of the report and HPX is presently carrying out works and it anticipates producing 20 million tons annually but rails to transport these ore remains a major challenge (LGS 2014).

2.4 Iron ore processing

Iron has special properties which make it useful for application in the everyday life. These properties include high strength, ductility, ability to conduct heat and electricity. While economic downturn reduces the demands for goods and services, so do the demands of metal but as the wheel turns the demand of metal also rises. To acquire the desired metal from the ore requires processing. There are several different methods proposed for iron ore processing but the choice for robust processing scheme of iron ore beneficiation relies on detailed characterization. Characterization is the process by which a data set that describes several different properties of the mineral sample is generated.

2.4.1. Iron ore characterization

Iron ore characterization is required for proposing potential method of beneficiation. Several techniques such as physical and mineralogical characterization can be used to study the sample. A range of issues surrounds the characterization and beneficiation of low-grade iron ore fines. These are high alumina content, poor liberation, and the generation of excessive fines because of

friable nature of the ore (S.S. Rath et al, 2014). These resources contain minerals such as limonite and goethite and they contain high percentages of volatile material. This loss on ignition decreases the strength in the subsequent sinter or pellet production. Another significant discovery of iron ore fine is that they contain three dominant textural types of goethite colloform, banded vitreous, massive vitreous and earthly or ochreous goethite (Das et al, 2010). Impurities such as Al, Mn, P, Si, V, Zn, and Co can be absorbed by the goethite minerals and these can decrease the sinter strength as they participate to the creation of different phases within the sinters (S. S. Rath et al 2014).

Physical and mineralogical characterization of iron ore sample can be obtained by examining the composition and structure of the sample (Zhang et al 2006). The composition will describe the chemical makeup of the sample while structure will reveal the crystal make up from atomic, subatomic, and microscopic arrangement of the atoms of the iron ore sample. The composition and the structure will dictate the properties of the iron ore sample, but both are somehow dependent on the processing of the iron ore (Rao et al 2013). Understanding the positions of atoms relative to one another in the iron sample will help closely understand the crystal structure. Furthermore, the nature of atomic bonding and diameter of atoms in the sample will all help understand the atomic structure. Hence, high-resolution electron microscopy and diffraction methods are possible means through which we can understand the structure.

2.4.1.1. SEM-EDX

The SEM is an electron microscope that uses electron beam to interrogate the sample to produce a morphological structure and grain appearance. It is equipped with the EDX which can assist in reveling the elemental presence of chemical element present in the ore sample. For determination

of composition or orientation of individual crystal or features, the SEM can be combined with EDX or EDS (Nuspl, M., Wegscheider, W., Angeli, J. et al (2004).

2.4.1.2. X-Ray Fluorescence Spectroscopy

This is an analytical method which relies on the interaction of x-ray with a sample to determine the elemental composition. In most cases, it is nondestructive and as such, it is suitable for solids, power, and liquid. The set up and configuration can determine the range of detectable elements but usually, the EDXRF can detect element from Sodium (Na) to Uranium (U) while the wavelength dispersive (WDXRF) can detect down to Beryllium (Be). X-Ray beam that hits the sample is either scattered or absorbed and if neither of the two occurs, the x-ray beam will be transmitted through the sample. When this occurs, the x-ray can interact with the atoms and this interaction can cause fluorescence and this fluorescence is used in the x-ray fluorescence method to study the sample. In addition, the x-ray can also scatter from the sample and this scattering light lead both to loss and no loss of energy. This is referred to as the Compton and Rayleigh scattering. Compton and Rayleigh scattering and transmission, the ratio of adsorption/ fluorescence depends on the sample thickness, density and composition and the energy of the x-ray. The basic process involves an incoming x-ray knocking an electron form one of the orbits surrounding the nucleus. A hole is then created in the orbit which leads to unstable higher energy state of the atom. To restore stability of equilibrium, another electron of higher energy drops in the lower orbital to fill the hole. The excess energy created by the falling of this atom is then emitted in the form of fluorescence x-ray. The energy difference between the expelled and replaced electron is characteristics of different atoms so the energy of the characteristic atom is causally linked to the element being analyzed. Equally so, multiple transition of expelling and

replacement is possible. In such case for a single element, there can be numerous about of XRF peak with variation of different peaks intensities (C.L.Luke 1968).

2.4.1.3. X-ray diffractometry

X-rays diffractometry (XRD) is a characterization technique used to discretely identify the crystallinity of a material. The XRD can identify phase composition, grain size, orientation, strain stage and other structural defect in crystal structure. Because it is noncontact and nondestructive, it can be used to carry out insitu analysis on samples. The basic concept of diffraction is the use of x-ray to interact with a sample and a detector is placed to record the intensity of the x-ray as counts or counts per second. A diffraction pattern is then generated consisting of peak intensity plotted against positions. Diffraction on sample can be done either on a single crystal or a powder. However, powder diffraction present plot of intensity of x-ray scattered by a sample while single crystal produces spot pattern. In powder diffraction, the detector moves in a circle about the sample and its position is recorded as the 2 theta (2ɵ). The detector then records the number of x-ray observed at each angle (2ɵ) which is usually recorded in counts or counts per second. The Bragg-Brentano Para focusing geometry is applied in many models of x-ray diffraction. In this model, the incident angle of the x-ray (omega) changes in conjunction with the 2 thetas to keep the x-ray beam properly focused. Rotating the x-ray tube or rotating the sample can accomplish the combined change mentioned. Because x-ray has approximately similar wavelength as compared to the interatomic spacing of atom and that they can scatter from atoms in a sample, they contain useful information about the atomic arrangement of the sample. When light is scattered by a periodic array with long-range order, diffraction will occur thereby producing constructive interference at the specific angle. Long range periodic arrangements of atoms help in characterizing crystalline samples. The diffraction

pattern produced is usually represented as a product of the unique crystal structure of the sample by different peaks which corresponds with of different 2 theta position and counts. The pattern calculation treats a crystal as a collection of crystal as a collection of planes of atoms. Every peak is attributed to scattering from a specific set of parallel planes of atom and miller indices (hkl) are used to identify the plane of atoms. To assist in analyzing the atomic and microstructure of the sample, the diffraction peaks can be related to the plane of atoms. The Bragg law ($\lambda=2d_{hkl}\sin\theta$) can be used to calculate the diffraction peak position as a product of interplanar spacing (Lev S. Zevin and Giora Kimmel 1995).

2.4.1.4. Mineral Liberation Analysis

Mineral liberation is one of the major steps in the separation of minerals of interest from their gangue associates. The importance and value of liberation analysis as applied to mineralogy and mineral processing has been discursively dealt with by several authors (R. Fandrich et al. 2007). The development of the mineral liberation analyzer (MLA) has found profound application in mineral processing and mineralogy (Fandrich et al. 2007) to determine the degree of liberation of ore from their gangue (Paul J. Sylvester 2019). Mineral Liberation Analyzer (MLA) self-possessed of a scanning electron microscope (SEM) . This MLA has the energy dispersive x-ray (EDX) spectrometers. The scanning electronic microscope has a computer software that is able to program microscope process and data attainment for computerized mineralogy (Paul J. Sylvester 2019). The MLA made its first appearance in the 1990s (Gu and Napier-Munn, 1997) and presented a discrete combination of BSE image analysis and x-ray mineral identification to provide quantitative mineral liberation characterization. The data set collected in the MLA has the collection of average mineralogy, absorbency, particle size and form, mineral group and digital textural maps can be collected on ores samples. The principle is based on backscattered

electron (BSE) image analysis for determination of x-ray spectra, grain boundaries and location of achievement and assemblage of distinctive x-ray bands of the mineral variations by evaluating them to the reference library of bands. Advantages of the MLA include the additional of monotonous toil-severe analysis by systematic, computer -automated analysis, the reduction of potential of operator error, large number of examined mineral grains for statistically representative analysis of the ore sample, the ability to distinguish fine grained or intricately intergrown minerals at micron scale, and etc (Sylvester, 2019). The MLA is unable to distinguish mineral of remarkably similar compositions (gypsum and anhydrite) and polymorphs (calcite-aragonite; rutile-anatase-brookite; kyanite-sillimanite-andalusite). Potential disadvantages of such method is the unobtainability of the directive character reference materials to reveal correctness .

2.4.2. Particle size effects

Particle size analysis determines the grinding quality and aid in setting up the degree of liberation for value mineral particles from the gangue minerals. During mineral separations, the size analysis is used to find out the optimal that will be fed to the process for maximum efficiency and reduce losses (Wills and Napier-Munn, 2006). Knowledge of these particles' size can improve the performance of the plant and help to reduce losses. Consequently, it is imperative to obtain accurate and reliable information on particle size distribution about the feed materials. Determination of particle size benefits well from collection and utilization of representative sample of the bulk sample that can be used in the assay. Acquiring quantitative data on particle size distribution in the material is the primary objective of precision particle size analysis (Bernhardt, 1994; Allen, 1997). In fact, it is impossible to measure the exact size and shape of an irregular particle. So, the term length, breadth width and thickness or diameter has

had relatively little meaning since there are many different values that can be measured. If the particle is a sphere, its diameter gives the definition of the size, and etc. but for irregular particle, it is of best practice to cite the particle's size in a single term of single quality, which is often described as the equivalent diameter. The equivalent diameter is the diameter of a sphere that behaves similar way like the particle when subjected to several specific processes. Equivalent diameters are usually dependent upon the technique of measurement therefore, the process to be controlled must be closely duplicated by the particle sizing method (Wills and Napier-Munn, 2006).

Even though there are a wide range of particle size analysis techniques, the Stokes' diameter, the Projected area and Sieve-aperture diameters are several common forms of equivalent diameters being measured now . Sedimentation and elutriation can be used to measure the Stoke's equivalent diameter while microscopic techniques can be used to measure the projected area diameter. The sieve – aperture diameter can be measured by the sieving techniques. Several equivalent diameters are commonly (Wills and Napier-Munn, 2006).

Test sieving is one of the highly essential techniques of size analysis due to its large uses in industry and science. It is a method of size analysis that renders finer particles (75 microns) as being in the sub sieve range even though modern sieves can allow sieving down to 5 microns. The oldest method for particle size analysis is the sieve method (Wills and Napier-Munn, 2006). It is accomplished by passing on a certain weight of materials repeatedly through a progressively finer sieves and then collect the retained materials on each sieve and weighting them to ascertain the percent of weight in each size portions. Sieving is accomplished wet or dry but during wet sieving, the material is typically disturbed to show the screen opening since the technique is complicated especially when treating irregular particles since particles with nominal size near the

size of the screen aperture may pass through only if they are orientated and presented to the opening in a favorable position (Wills and Napier-Munn, 2006). Longer sieving time will lead to the exertion of undue large weight of material on the screen and enough small particles may find their way through the sieve. The availability of near size particles creates blinding of the screen openings and lead to obstructions which affects the efficiency of the screen and this issue is common with an excessively small aperture sizes. The process of sieving is done in two forms, elimination of particles that are considerably smaller than the aperture, and the separation of the near size particle (Wills and Napier-Munn, 2006). The mass of materials on the screen (charge) and the way motion is imparted to the screen can also determines the effectiveness of the sieving process. The choice of sieve size is influenced by a consecutive relationship between the aperture of successive sieves. Generally, if the sieve ranges are selected correctly, no more than 5% of the materials will be reserved on the coarse sieve or still go beyond the finest sieve (Wills and Napier-Munn, 2006). More accurate work can lower this limit. The test sieving method is usually accomplished by machine sieving as hand sieving is tedious and results in inaccurate data. The result from the sieving test can be tabulated and presented in several different ways. However, there are several most adopted ways that they can be tabulated (Anon.,1989). To find out the full significance of the results, it is always important to plot the result of the sieving test graphically as cumulative undersize or oversize against particle size (Napier-Munn et al., 1996). The median size range is an important quantity that can be determined from the graph. This fact is the mid-point in the size distribution that 50% of the particles are below this size and 50% are above this size. Frequently, the plot takes an S -shape showing a congestion of data at the extreme of the plot. There are several plotting methods to proportion the ordinate but for communication studies, non-uniform distribution of particle sizes is obtained using the Gates-Gaudin-

Schuhmann (Schuhmann, 1940) and the Rosin- Rammler (Rosin and Rammler, 1933-34) methods (Wills and Napier-Munn, 2006). These methods turn to equations for representation of particle size which lead to a more than a linear scale in one region and constructed in another.

The Gate-Gaudin-Schuhmann methods plot the cumulative undersize datum against sieve aperture on a log-log axis. Because most log-log plots lead to straight line, interpolation is much easier. Limited number of sieves can be utilized to examine the important aspects of the size distribution when the analysis yields a straight-line graph as this reduces the burden of routine analysis. In the cumulative undersize curve, the log-log scale will considerately expand the region below 50% mainly that below 25% while it tends to harshly contract the area above the 50% mainly above 75% which is the main drawback of the method (Wills and Napier-Munn, 2006).

The Rosin-Rammler method is used to plot sieve analysis data obtained from particles of a ball mill. It is given as 100- P = 100 exp(bdn), where P - cumulative undersize in the percent, b - constant, d -particle size, and n - constant. This statement can be expressed as Log [ln 100/100-P]=logb +nlogd. Hence, a plot of In[100/(100 - P)] versus d on log-log axes provides a line of slope n. The log-log technique enlarges the regions below the 25% and the 75% cumulative undersize and contract the 30%-60%. It has been stated that this reduction is not sufficient to generate severe adverse effects (Harris,1971).

Of the two methods for plotting results from the sieve analysis, and in mineral processing application, the Gates-Gaudin-Schuhmann plot is likewise termed the Rosin-Rammler method though Harris (1971) has suggested that the later method is of better performance in mineral processing applications. However, Allen (1997) noted that the later method should be utilize with caution because taking log always reduces scatter and taking log twice is not advisable .

2.4.3. Comminution

Comminution is the general term given to the crushing and grinding of mineral particles to liberate them from their gangue associate (Wills and Napier-Munn, 2006). It is the reduction of the physical dimension of materials from run-off mines. The objective of comminution is to unlock composite mineral grains in raw ore into a more independent mineral grains and to adjust the size of minerals particles to adapt to the optimum size for the successive separation process. Comminution is carried out in mineral processing in two stages: crushing and grinding. Crushing is the first stage of the comminution process. Because run-off mines usually come in sizes in range of 200 mm down to 150 mm, crushing operations are carried out on these materials to reduce them further down to 10 mm or 5 mm to a level that grinding can be conducted. Two mechanisms are available for crushing operations are compression of the ore materials next to a inflexible surface or physical exertion of effect on the ore alongside a surface rigidly constrained motion path. Both mechanism of crushing is carried out dry and in numerous distinct stages, with little reduction ratios, varying from 3to 6 in each stage. The crushing stage reduction ratio can be termed as the ratio of maximum particle size arriving to maximum particle size exiting the crusher, though additional meanings are occasionally used (Wills and Napier-Munn, 2006). Crushing in mineral processing operations are done by crushers. In contrast to crushing, grinding is achieved by abrasion and ore's impact by the free motion of isolated media which include rods, balls, or pebbles.

The theory of comminution holds that stress distribution in rocks depends on the existence of defects or weaknesses with in the matrix and cracks sites acts as area of stress concentrations (Barry A. Wills, Tim Napier-Munn, 2006). The comminution principle is further focused on the

energy input that yields certain particle size created. The theory assumes that all materials are brittle and as such no energy lost to contraction or expansion. The wide variation of particle size and shape in feed and product and because there are some wastages of energy as heat and sounds that cannot be determined exactly, there is no possible way to find out the accurate amount of energy required to affect size reduction of a given materials (Barry A. Wills, Tim Napier-Munn, 2006). Kicks, Rittinger and Bonds have proposed several laws to help determine the energy consumed in comminution (creation of new surfaces). In most part, these laws do not consider the mechanical losses in the crushers but more concerned about the creation of new surfaces. Hardness, temperature sensitivity, moisture content, reduction ratio, mode of operation, energy used in comminution, and cost are major factors that affect the comminution(Barry A. Wills, Tim Napier-Munn, 2006).

Major size reduction machines are crushers (coarse and fine) they comprise of jaw, gyratory cones and crushing rolls. These machines accept feed materials of 250 to 150mm and break them down into particles of 50-5mm in size. Intermediate crushers comprise of roller mill, granulator , hammer mill and they accept feed size of 50- 5mm and produce product on 5-0.1 mm. Fine crushers are also called grinders. They comprise of attrition mills, tumbling mills, rod mills, and ball mills. Their feed is in range of 5-2 mm and product size is in range of 200 mesh. Ultrafine grinders comprise of fluid energy or jet mill , fines impact mill and they receive feed less than 6mm and give product in range of 1 to 50 microns (Barry A. Wills, Tim Napier-Munn, 2006).

The selection of a size reduction equipment is based on the following: ability to produce desired size and shape, accept maximum input size expected, have large capacity, not choke, ability to pass unbreakable materials without causing damage to itself, small power per unit weight of

product, resist abrasive wear, have prolong sieving life, easy and safe to operate and easy access to internal parts for maintenance (Barry A. Wills, Tim Napier-Munn, 2006).

2.4.4. Gravity Separation

Gravity separation is a method of separation that uses difference in gravity of minerals to separate them in a fluid medium. It has been applied to treat different varieties of ore at particles sizes below 50 microns. The swell cost of flotation reagents associated the careful upgradation of low-grade complex with caused the method to decline in the opening half of the 20^{th} century . The ore and their environmental suitability have caused the methods to be reevaluated and applied at various mines across the world (Wills and Napier-Munn, 2006). This method can be great advantage when applied to coarse size immediately after liberation and will yield for subsequent treatment phases owing to diminished exterior area, exceedingly successful dewatering and etc. The Theory of gravity concentration is more concerned with having a mark difference within the gravities of both minerals to be separated . A term called concentration criterion is used to tell the suitability of gravity separation application to a material (Wills and Napier-Munn, 2006). The concentration criterion is defined as (Dh-Df/Dl-Df) where *Dh* – relative density of dense mineral, Dl -relative density of light mineral, and Df – relative density fluid medium. In typical terms , once the quotient of the concentration criterion is large negative or positive, there is a high suitability of gravity seperation and if it's the other way round, the chance of gravity application is marginal(Barry A. Wills, Tim Napier-Munn, 2006). Because the gravity process takes place in a fluid medium, the process is influenced by the size of the particles and their motions in the fluid medium. Larger particles will have better effects as compared to smaller particles, so it is recommended that the particles be sufficiently coarse to obey motion according to Newton's law. To reduce the size effects and render the process of

gravity separation relatively dependent on motion of the particles specific gravity, it is important to closely size and control the feed. Clarity of the gravity concentration and conspicuous cut-point can be reduced due to the rise in the viscosity and the existence of slime. Consequently, it is essential to eliminate all particles below or about 10microns on or after the gravity separation feed although this removal may lead to lost to the tailings. De-sliming is important since the gravity process is overly sensitive to the presence of slimes (Wills and Napier-Munn, 2006). There are several different form of gravity separators ranging from jigs, spirals, shaking table , duplex concentrator and pneumatic tables etc. The shaking table utilizes the flowing flick efficiently to isolated thick light load particles from small flattened particles and this is probably the most metallurgically effective form of the gravity concentrator. The normal size range for riffled tables or sand table is in the range of 3 mm to 100-micron meters

2.4.5. Magnetic seperation

Magnetic separation utilizes the difference in magnetic properties of different materials to separate value minerals from gangue miners. Every material responds differently when placed in magnetic fields. Due to these responses, materials can be categorized into two different classifications corresponding to how they are drawn or repelled. Diamagnetic materials repel the line of magnetic force to a point that the magnetic field intensity is slight because the force concerned is comparatively little so diamagnetic substance are unable to be concentrated magnetically. Paramagnetic materials are stuck alongside the lineup of magnetic force point where the field strength is strong so they can be concentrated magnetically. Hematite (Fe_2O_3) Ilmenite ($FeTiO_3$), rutile (TiO_2), pyrrhotite(FeS), chromite ($FeCr_2O_4$) and manganese minerals are few examples of paramagnetic minerals. O, Ni, Ti, Co, Cr, Mn, Ce, and the Pt group metals are some elements that are paramagnetic in nature but the occurrence of iron in several

ferromagnetic manner attributes to the paramagnetic properties of minerals. A special case of paramagnetic involving extremely high susceptibility to magnetic forces is called ferromagnetism (Wills and Napier-Munn, 2006). Ferromagnetic materials possess excessive magnetic force susceptibility, and they keep some magnetism even when they are taken away from magnetic field . This is called remanence. Because they are highly magnetic, they can be concentrated by low-intensity magnetic separator. Magnetite (Fe_3O_4) is the principal ferromagnetic minerals however, hematite (Fe_2O_3) and siderite ($FeCO_3$) can be heated to create magnetite.

2.4.6. Flotation

The most versatile and important mineral processing method is undoubtedly Flotation (Wills and Napier-Munn, 2006). Though initially designed to treat sulfide minerals, its application is continually being expanded to treat greater tonnages of different kinds of mineral including iron ore. Flotation is a physico-chemical separation method that utilizes difference in superficial properties of value and undesirable materials. The theory of flotation is a multifaceted one as it involves three separate phases (froth, solids and , water) with numerous sub-procedure and connections that are not totally well understood. According to Wills and Napier-Munn (2006), three mechanisms are responsible for the recovery of materials by flotation. Selective attachment of mineral particles to air foams (true flotation) , entrainment in water that goes into the froth, and physical cut-off amid particles in foam attached to air foams (referred to as aggregation). In direct flotation the value mineral particle is floated while the unwanted mineral is depressed. The opposite is reverse flotation. The froth stabilizes and improve the general selectivity of the flotation course.

The connection between the grade and recovery is a trade-off that is compulsory to be taken care off in line with working restraints and that is combined in the managing of the best froth stability (Wills and Napier-Munn, 2006). Air bubble attach to hydrophobic water repellent particles and travel up to the froth phase. If the froth is stable, the air bubble will support the mineral particle then, they will rupture and release the mineral particles. To attain this, several chemical adjectives called flotation reagents are used (Tülay TÜRK et al 2019, Somasundaran et al , 1964).

The contact angle between mineral particles and bubbles in water help determines the surface relations to flotation reagent and this relies on the forces that works on that surface (Collectors are flotation reagents that impact hydrophobicity to minerals particles. Floaters helps to keep the pulp stable. Depressants help to depress hydrophilic mineral particles while activators activities the active site of the mineral surface to make it possible for collectors and depressants adsorption. The alkalinity of the pulp plays an particularly significant part in the regulation of the flotation process as it tends to control selectivity in complex separation and balance the relations between reagents concentration and pHs (Wills and Napier-Munn, 2006).

2.4.7. Pyrometallurgy

The branch of metallurgy that studies with ores as raw materials and metals as finished product is called extractive metallurgy Habashi, 1997). Pyrometallurgy is a branch of extractive metallurgy that is more concerned about the thermal treatment of minerals, ore, and their concentrates to create physical and chemical transformations in the materials to enable good recovery of value metals. The production of pure metals, intermediate compounds, suitable feed for processing and alloys can be a result of this thermal treatment process (Habashi, 1997). Pyrometallurgy is an easily adaptable method for extraction of metal. Physical and metallurgical

properties are evaluated to understand the iron ore metallurgy. The physical properties will give an indication of the minerals behavior during handing in the furnace while the metallurgical properties will give indication of the mineral behavior during the reduction process (Habashi, 1997). The choice for selecting iron ore for steel production is affected by some properties such as tumbler, graze and ruin indices, absorbency, chemical configuration, loss on ignition, reduction performance and thermal degradation (Kumar et al, 2008).

2.4.7.1 Reduce roasting

Roasting is the first step in the iron ore metallurgy. Roasting involves the heating of the ore in air to remove water, decompose carbonates into oxide and convert sulfides into oxides (Habashi, 1997). Oxides are later reduced in a blast furnace in which roasted ore, coke, and limestones (impure $CaCO_3$ are introduced). All different iron ores- Hematite Fe_2O_3 , Magnetite Fe_3O_4 , Goethite Fe_2O_3 .H_2O and Siderite Fe_2O_3 $FeO.CO_2$) all have oxygen in their chemical formula. The addition of carbon is essential in the reduction process : $2Fe_2O_3$ (s) + 3C(s) → 4Fe(l) + $3CO_2$ (g). Fe_2O_3 (s) + 3CO(s) → 2Fe(l) + $3CO_2$ (g). $CaCO_3$ (s) → CaO(s) + CO_2 (g). CaO(s) + SiO_2 (s) → $CaSiO_3$ (l).

2.4.7.2. Reduction of iron oxide: Chemical Aspect

The complete iron oxide reduction occurs at an appreciable rate and only at temperatures above 900^oC (Habashi, 1997). Below this temperature range, reduction is usually incomplete. The general reduction follows the form Fe_2O_3 to Fe_3O_4 to FeO and Fe. However, reduction of iron oxide below the Curie temperature (570^oC), the reduction follows the scheme Fe_2O_3 to Fe_3O_4 to

Fe because FeO is unstable below 570^{o}C. A metallographic examination usually depicts a layered structure when a hard-dense oxide is reduced and show Fe_2O_3 in the core surrounded by Fe_3O_4, and FeO (Habashi, 1997). However, for absorbent oxides no distinctive boundaries are seen, apart from a continual conversion from Fe on the external to Fe_2O_3 in the center due to faster reducing gas penetration and reaction at any oxide interface. Ferric oxides Fe_2O_3 has higher reduction velocity than Fe_3O_4 . In the similar manner, hydrogen is more effective as reducing agent than CO. The percentage of reduction is affected by sluggish periphery strata of gas which encircles the oxide particles which is like the nature of heterogeneous reactions (Gaviria et al, 2007). This is dependent on the drift rate of the reducing agent gas preceding the oxide particles implying it is dependent on the layout process and reduction mechanism (Habashi, 1997). Increasing the gas flow rate may eliminate the resistance of the boundary layer but his is uneconomical since unreacted gases will flee in the heap or be taken over of dust particles of excess (Habashi, 1997).

2.4.7.3. Reduction of iron oxide: Technical aspect

In the 14th century, furnace was developed to produce iron. They were also built to melt iron to produce pig iron that could be trapped from the furnace in a liquid form, hence permitting sizeable amount of production of constant operation. Such furnace is called the blast furnace because it utilizes blast air. The current practice involves the transfer of nearly all pig iron in liquid state to steelmaking factories and in this form, it is termed hot metal. Sporadically, it is of material in soil form for some useful distributing and it is cast into container where it coagulates to form what is termed pigs. The practices that take place in the furnace are reduction of the iron

compounds existing in the ore, and isolation of the subsequent iron from the slag (Habashi, 1997).

2.4.7.4. Reduction of iron oxide: Direct reduction

The reduction of iron oxide typically happens in a blast furnace by either carbon or by carbon monoxide that are formed from carbon gasification. Direct reduction is the term used to describe the reduction method conducted by carbon and is described by the following equation FexOy+yC= xFe+yCO (Ünal et al, 2015). Indirect reduction is also the term used to describe the reduction process conducted with CO and the reaction that describes this process is given as $FexOy+yCO=xFe+yCO_2$ and $yCO_2+yC=2yCO$ (Boudouard Reaction) (Ünal et al, 2015). Ünal et al (2015) have also shown in that hydrogen can be used to indirectly reduce ferrous materials and it follows the equations: $3Fe_2O_3+H_2\rightarrow 2Fe_3O_4+H_2O$; $Fe_3O_4+H_2\rightarrow 3FeO+H_2O$ and $FeO+H_2\rightarrow Fe+H_2O$. This process is a gas to solid reaction that occurs in two or three stages. In the case of temperature greater than 570°C, hematite (Fe_2O_3) primarily get converted into magnetite (Fe_3O_4), then into wustite (Fe1-yO) and in the end into metallic iron. On the other hand, for temperature below 570^oC, magnetite is strictly converted into iron since wustite is not thermodynamically secure (Ünal et al, 2015). It is possible to produce iron from its ore by direct reduction using coal based or gaseous agents as reducing agents which are termed direct reduced iron (DRI) or sponge iron. Since DRI acts as a ideal replacement of scraps for steel fabrication in electric arc furnace, basic oxygen furnace and etc., they have discovered a rapid global expansion in their fabrication. DRI can be of solid form or pellet form and they are a solid-state product. Increase in supply of non-coking coal, the shortage of coking coal bank and manufacturing significance of DRI have preceded to many undertakings on the growth of several direct reduction methods (Wagner et al, 2006) .

2.4.7.5. Complex oxide reduction

To determine the most suitable operating conditions for direct reduction reactors, it is necessary to understand the kinetics of reduction of iron ore to iron. The reduction reaction is overly complex since it involves several elementary reactions, and several multiple reactions can occur simultaneously (Bessières et al, 1980). They show the different possible ways that the chemical kinetics of the single, double, and triple reactions can be determined. This is done by the help of a reactional triangles depending only on the nature of the different reactions that are taking plac

CHAPTER THREE

MATERIALS AND METHODS

3.1. Sample collection and preparation

A low-grade iron ore sample was collected and shipped from Gangra mines, in Nimba Liberia. The sample was crushed to below 2 mm using a laboratory jaw crusher. The sample was ground using a conventional laboratory ball mill and screened using a laboratory screen. A representative sample of 1000 g was collected, and mechanical sieve analysis was conducted based on ASTMD 422- Standard Test method for particle size analysis of the low-grade ore sample. After sieving for 10 minutes, different weight fraction of materials was collected from different sieve sizes, weighed and recorded and a mass loss was 11.1 g was observed.

3.2. Sawdust Preparation

Waste sawdust was collected from a local sawmill in Galadimawa, Abuja Nigeria. It was sun dried for 4 hours to reduce water and other impurities. The sawdust was sieved to obtain a desirable size fraction (1 mm to 150 microns). 120 grams of sawdust was measured and

compressed into a fireclay crucible and placed into a carbonite at 10 ramp rates furnace and heated for 1 hour at 500^{o}C . This temperature range was chosen to avoid the sawdust converting into ashes as the nitrogen flow rate was controlled in line with the temperature to prevent the conversion and this also is consistent with the literature (Lam and Zakaria 2008) . After 1 hour, the sample was collected from the furnace, cooled down and weighted. This process was repeated till the needed amount of carbon for the reduction process was prepared. Following that, a sample was collected for SEM and EDX analysis to determine the percentage of carbon and other contents.

3.3. Reduction Roasting and Magnetic separation

Before reduction roasting and magnetic separation, dry magnetic separation was conducted on the as-received ore sample to determine the ore's response to a magnet. Following that, reducing roasting of low-grade iron ore sample was done in a laboratory muffle furnace by the aid of a high-quality refractory crucible. Several reactions are involved in the complete reduction of hematite to magnetite. A balanced stoichiometry reaction as shown in Equations 1 to 4 in section 4.9.1 were used to determine the theoretical amounts of carbon required to carry out the reduction process at the various temperatures. As a result, 10 gram of carbon was chosen to be mixed with 565.1 grams of raw ore. For the process, the powdered carbonized sawdust was uniformly mixed with the low-grade iron ore for a period of 2 minutes to ensure proper mixing. Thereafter the mixture was placed into furnace and allow to roast for different temperature ranges (750^{o}C, 850^{o}C and 950^{o}C) for 30 minutes and 50 minutes while keeping the carbon content in the mixtures constant. Consistent with the literature, this temperature range were chosen as favorable for hematite to magnetite transformation (Rath et al 2014, Gao et al, 2018).

After each round of roasting, the furnace was put off and the temperature allow to cool. After cooling, the crucible was removed from the furnace. Each cooled mass was collected and subjected to low intensity dry magnetic separation. Roasted ore products were subjected to low intensity dry magnetic separation. The investigations are presented in the flow diagram in *figure 3.1*

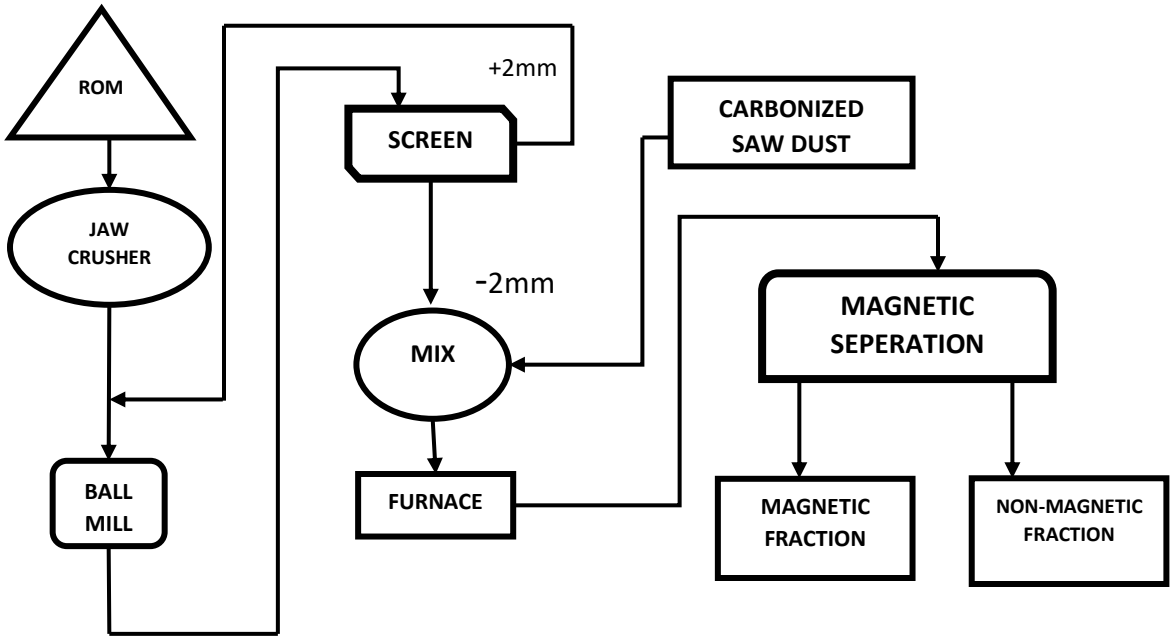

Figure 3.1: Experimental set-up of reduction roasting and magnetic separation

3.4. Characterization

The as-received sample was collected for XRD and XRF analysis before reduction roasting. Thereafter, the samples were collected form the individual roasted products for XRD analysis.

The products of magnetic separation were also taken for chemical analysis to determine the assay for the product.

CHAPTER FOUR

4.0. RESULTS AND DISCUSSIONS

4.1. Particle size distribution

Sieve No. Inch	Sieve Size (mm)	Wt. Retained (g)	% Wt Retained	% Wt. Passing

0.530	14.0	71.3	7.2	92.8
4	5.00	195.3	19.7	73.1
6	3.35	44.2	4.5	68.6
10	2.00	50.6	5.1	63.5
16	1.18	47.5	4.8	58.7
30	0.60	70.4	7.1	51.6
40	0.425	53.5	5.4	46.2
50	0.30	73.7	7.5	38.7
70	0.212	100.3	10.1	28.6
100	0.150	97.4	9.8	18.8
200	0.075	117.1	11.8	7.0
Receiver	< 0.075	67.6	6.8	0.2
Total		988.9	99.8	

Particle size distribution of as-received ore is shown in Table 4.1 with summary of analysis based on USCS classification size ranges. Particle size distribution in the as-received samples ranges in five divisions namely fine-grained gravel size, coarse grained sand size, medium grained sand size, fine grained sand, and fines material. The fine-grained gravel size material (Sieve No.4, 6 & above) –constituted 31.4%. The coarse-grained sand size material (Sieve No. 10) constituted– 5.1%. The medium grained sand size material (Sieve No. 16, 30 & 40) constituted – 17.3% and the fine-grained sand material (Sieve No. 50, 70,100 & 200) constituted – 39.2%. The fines material (Clay & Silts size material (Receiver) constituted – 6.8% summing a total of – 99.8%. The graphical depiction of the particle size distributions is shown in *figure 4.1*.

Table 4.1: Sieve analysis of unroasted ore sample

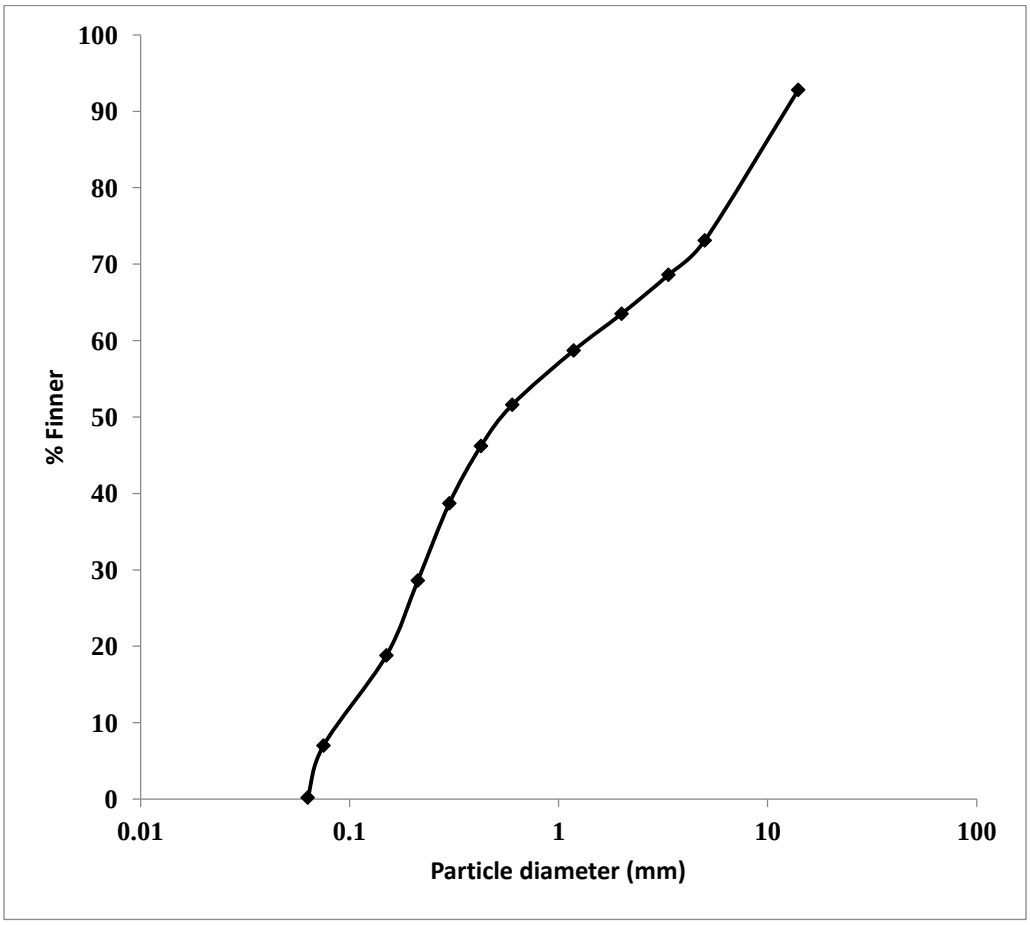

Figure 4.1. Particle size distribution for unroasted ore

4.2. Chemical analysis

The chemical analysis of the raw ore is shown in Table 4.2a. The sample contains 63.1% Fe_2O_3, 25.4% SiO_2, 9.1 % Al_2O_3, 0.7 % Cl, and 0.4 P_2O_5. LOI is 1.3%. It can be observed that the silica content is higher than the alumina content. The ore is composed of hematite, goethite, and silica.

Table 4.2.a Chemical composition of unroasted low-grade ore (mass %)

Compound/Element	**Fe_2O_3**	**Al_2O_3**	**SiO_2**	**Cl**	**P_2O_5**	**LOI**
Wt%	63.102	9.121	25.381	0.669	0.419	1.308

The characterization of sawdust as presented in Table 4.2b agrees with the literature as many sources have parallel results (Lam and Zakaria 2008). There was an observed minute discrepancy in the values of the properties measured as compared to the other results in the literature, but the difference is not significant to cause adverse result. Many other sawdust results in the literature have fixed carbon content between 40 to 57% which is in line with Table 4.2b. *figures 4.2a and b* present the EDX and SEM respectively while Table 4.2a shows some characteristics.

Table 4.1b: Characterization of saw dust

No	Properties	Value	Unit
1	Mean particle size	500	µm
2	Bulk density	0.23	g/cm3
3	Moisture content	9.25	%
4	Ash content	1.7	%
5	Volatile matter	81.85	%
6	Fixed carbon	7.2	%
7	Total carbon	54.3	%
8	Sulphur	0.01	%

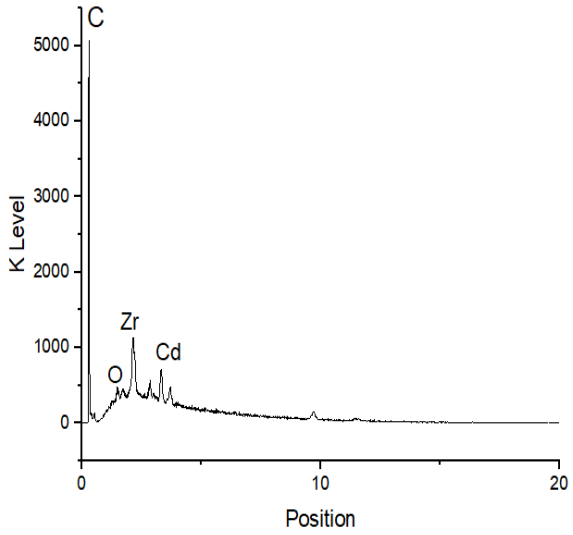

Figure 4.1 a: EDS estimate of carbonized

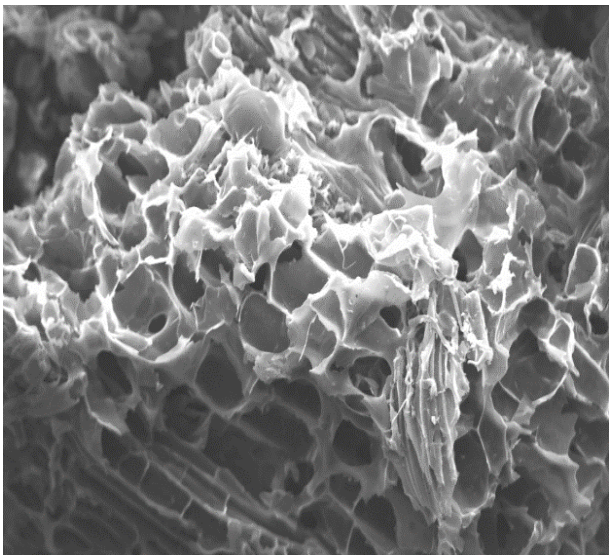

Figure 4.1.b: SEM image of carbonized sawdust

4.3. SEM AND EDS

The scanning electron microscopy was used to obtain information of the morphology and nature of the mineral grain size in addition to the sieve analysis. As shown in *Figure 4.2*, it can be observed that the particles of the unroasted sample appear more spherical. This can be attributed to excessive fragmentation in the ball mill. Energy dispersive spectroscopic shown in Figure 4.3 gives an estimate of the of the presence of iron and silica as dominant materials in the sample.

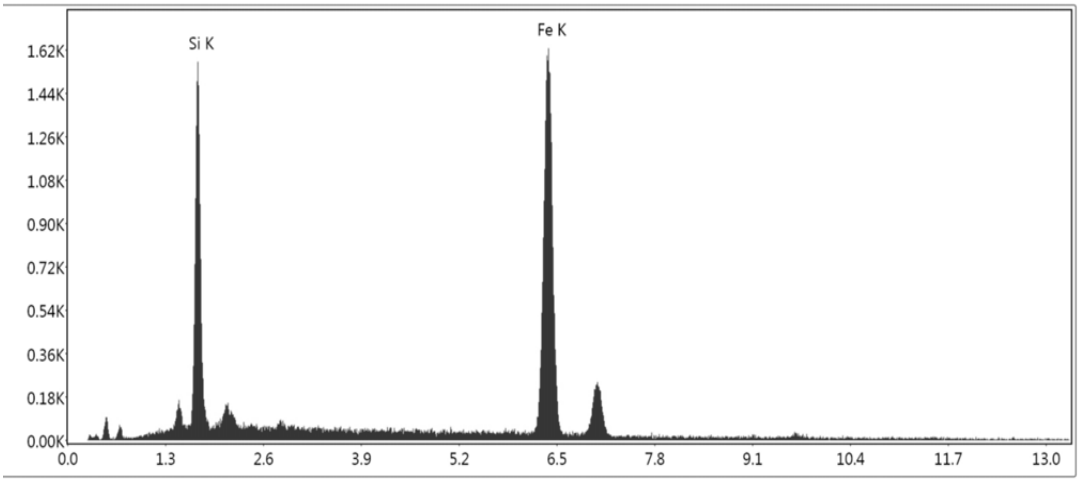

Figure 4.2: EDS plot for unroasted sample

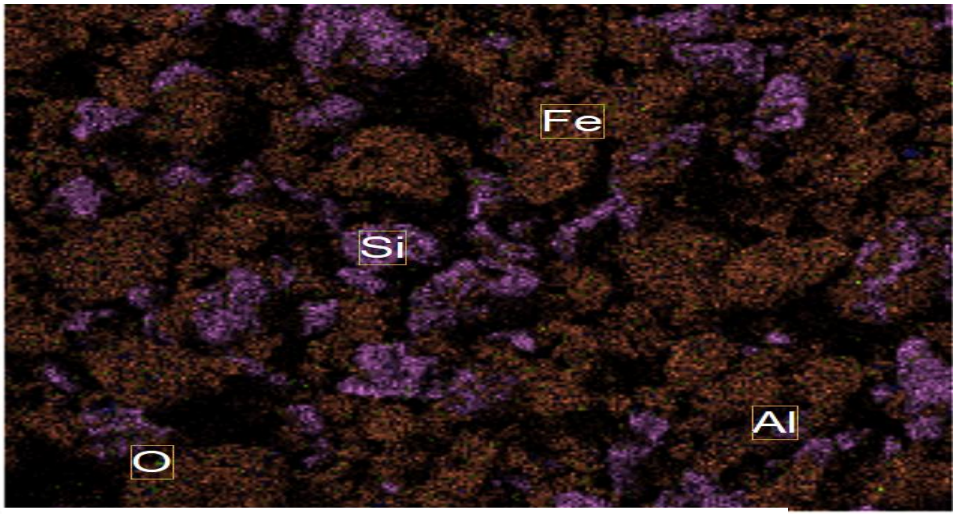

Figure 4.3: EDS Mapping for unroasted sample

The SEM images shown in *figure* 4.4 of the unroasted ore sample shows hematite dispersion within the clay and silica matrix. As shown in *figure* 4.3. Tthe EDS mapping reveals that the unroasted ore is predominantly composed of 64.% iron , 17% silica, 9% alumina and 8% Oxygen.

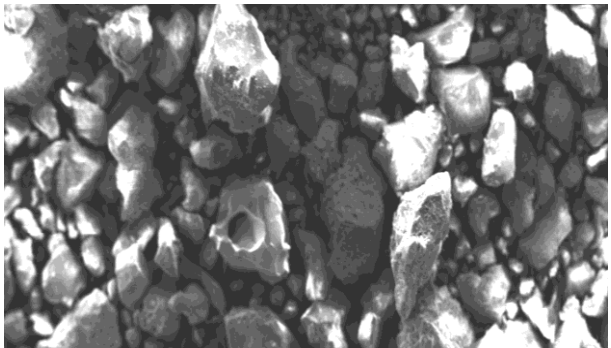

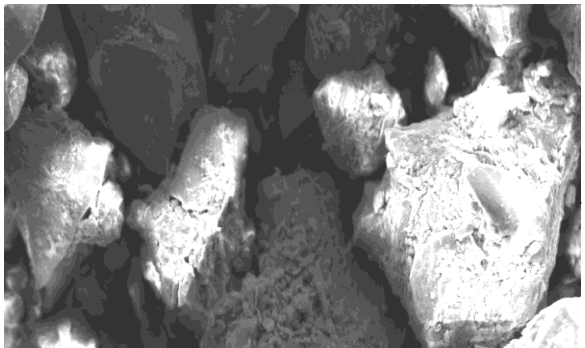

4.4. Phase composition

The x-ray diffraction study of the unroasted ore sample is shown in *figure 4.5*. The diffraction pattern indicates the presence of hematite, quartz, and goethite assemblages in the low-grade iron ore sample. These are the phases present in the unroasted ore sample. The magnetic susceptibility of hematite and goethite are exceptionally low as compared to iron minerals such as magnetite due to this the raw ore responded poorly to magnetic as the magnetic fraction obtained after subjecting 561.5 g of raw ore sample to dry magnetic separation was 50 g (9%).

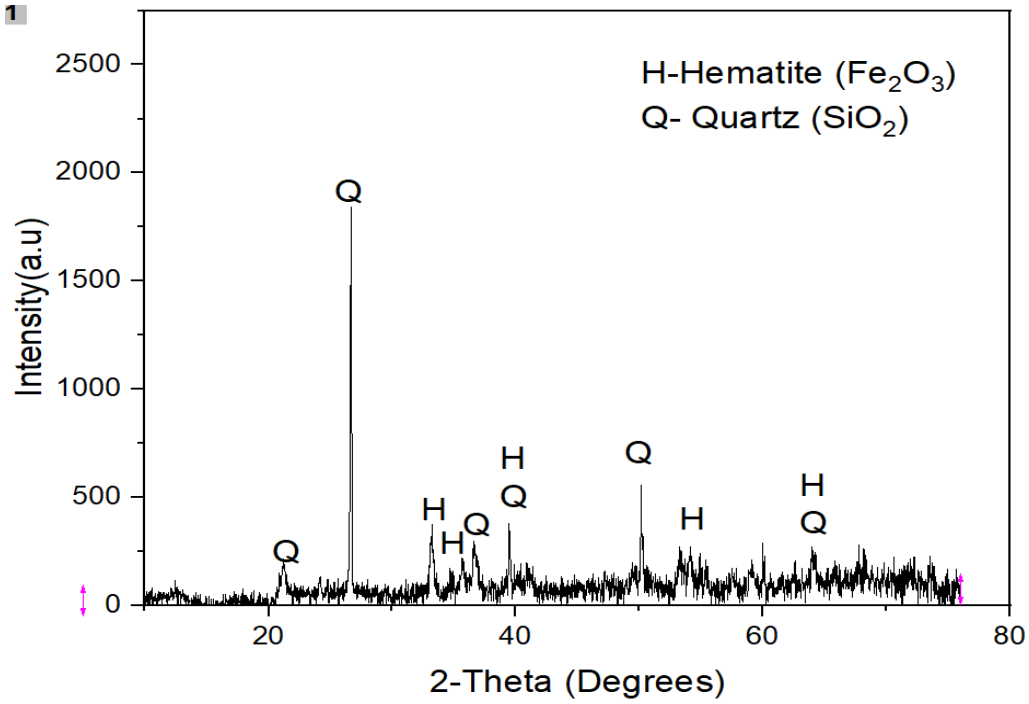

Figure 4.5 : X-ray diffraction for unroasted low-grade iron ore sample

The XRD pattern shown in figure 4.5 confirms that low grade iron ore sample from Nimba Liberia is dominantly composed of hematite and partially of silica and goethite. Temperature had a pronounced effect on the roasted products.

4.5. Effect of Roasting Temperature

Temperature has a profound effect on the weight of magnetic fraction and non-magnetic fraction after the magnetic separation. The carbon content or dosage for the ore was kept constant at 13.5g of carbonized sawdust mixed with 565.1g of raw ore sample. As shown in figure 4.6a and b for the 30- and 50-minutes roasting , the weight of the magnetic fractions increases sharply with increase in temperature up to 850^{o}C and above 850^{o}C up to 950^{o}C, the

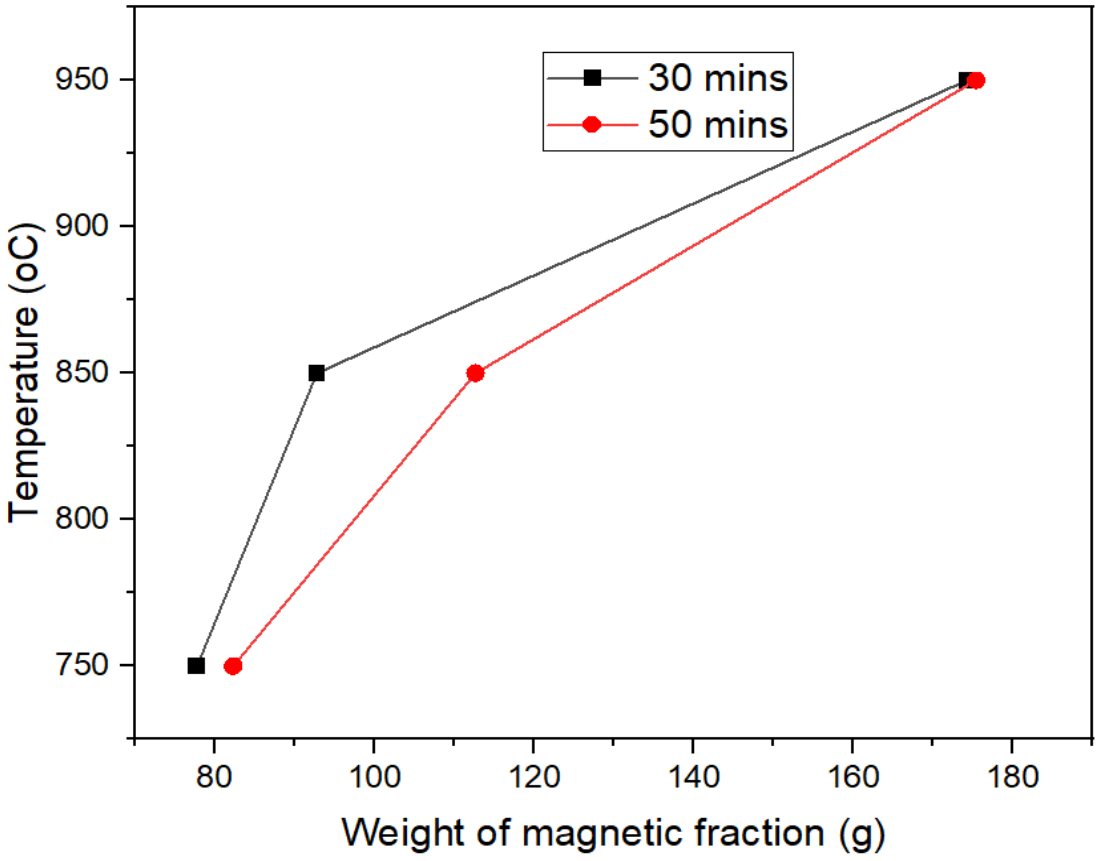

Figure 4.6. Effect of temperature on weight of magnetic fractions

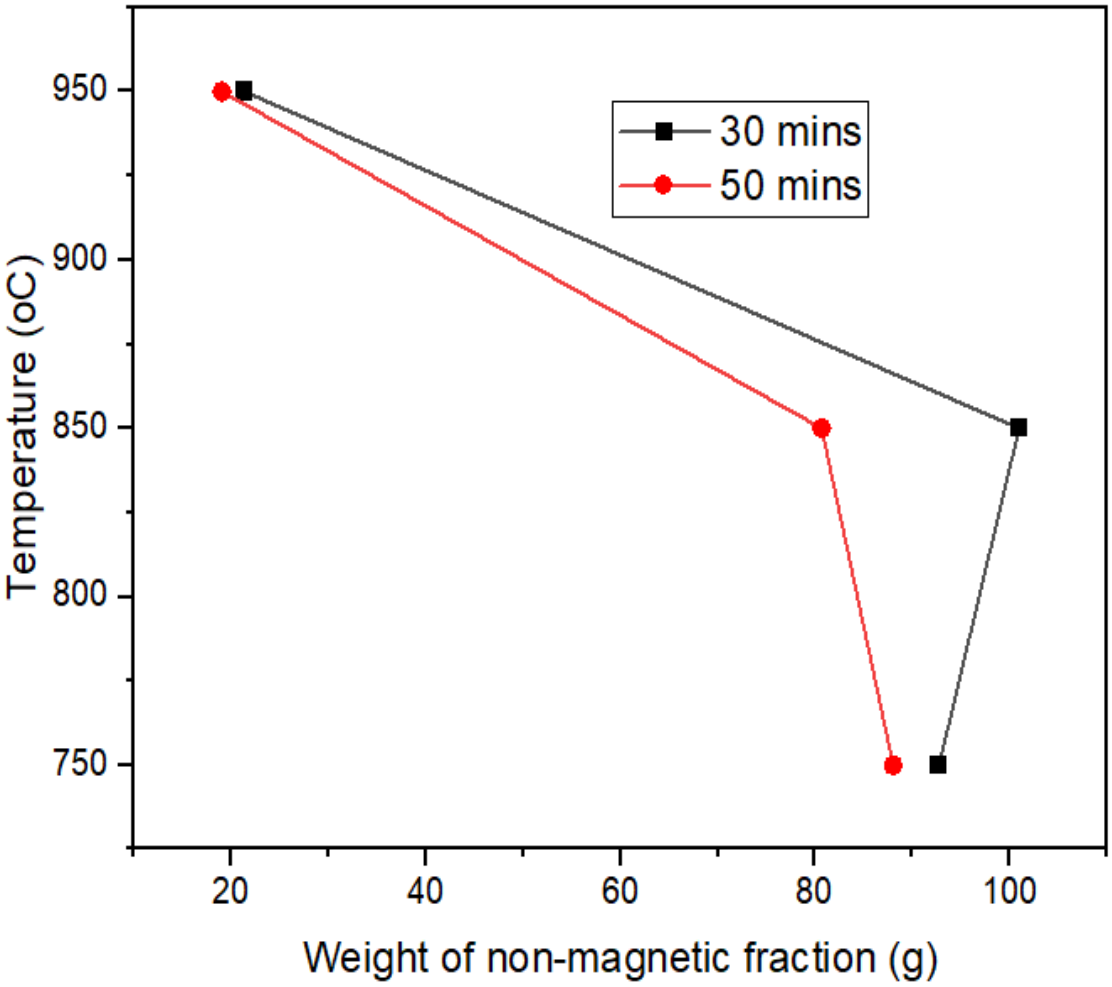

Figure 4.6b. Effect of temperature on weight of non-magnetic fractions

weight of the magnetic fraction increases gradually till the full temperature range. The relationship between the increase in temperature and magnetic fraction is linear and exhibit a positive slope for temperature between 850^{o}C to 950^{o}C. The reverse of this relationship is observed for the case of the non-magnetic fractions. The weight of the non-magnetic fractions

decreases progressively with increase in temperature from 950^{o}C to 850^{o}C. Below 850^{o}C to 750^{o}C, the weight of the non-magnetic fractions began to decrease gradually. The relationship between temperature and weigh of non-magnetic fraction is observed to be linear and showed a negative slope for changes in temperature from 750^{o}C to 950^{o}C.

Consequently for 13.5 g of carbon dosages added and mixed with 561.5 g of low-grade iron ore, the roasting process for reduction of hematite to magnetite occurs at several different temperatures. For temperature of 850^{o}C, the roasting process favors increase in weight of magnetic fractions for temperature range between 750 ^{o}C to 850^{o}C for 30 minutes roasting time and for 50 minutes roasting time, the increases in weight of magnetic fractions are favored above temperature range of 850^{o}C to 950^{o}C.

The increase in temperature causes an effect on the reduction of weight in non-magnetic fractions. From 950^{o}C to 850^{o}C, the reduction in weight is large with increase in temperature but less for temperature ranges from 850^{o}C to 750^{o} C.

4.6. Effect of Roasting time

Roasting time was studied to understand its effect on weight of the roast product. As can be seen in *figure 4.7*, the weight of the mixed ore that was roasted reduced as the roasting rounds were completed. The reduction in weight of each round of roasting for the 30 minutes period experienced 0.31 g, 0.54 g and 0.76 g reduction each for the three rounds of roasting conducted at 750^{o}C, 850^{o}C and 950^{o}C for 30 minutes each. The total of 561.5 g of mixed feed was roasted and the roasted product yielded 344.86 g of magnetic fraction and 215.03 g of nonmagnetic fraction with 1.61 g (0.28%) reduction in weight of feed due to total roasting time of 90 minutes.

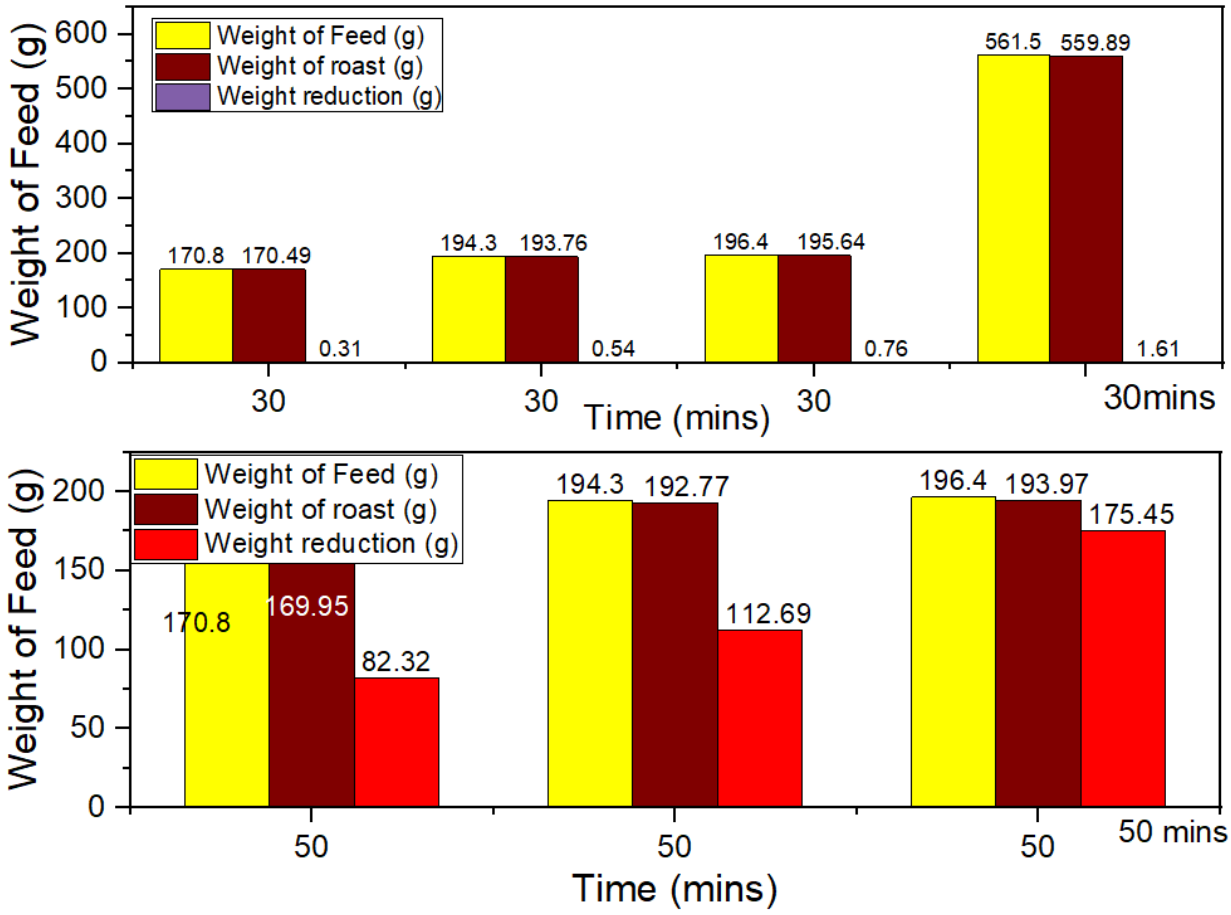

Figure 4.7: Effect of roasting time on weight of roasted ore

As shown in *figure 4.7*, roasting time also shows impact on the weight of the roasted product. The weight of the roasted ore products was different from the initial weight of the mixed unroasted feed. The reduction in weight of roasted products were 0.85 g, 1.53 g, 2.43 g respectively that were lost to roasting for the 50 minutes rounds of roasting. A total of 561.5 g of mixed ore was roasted and 370.46 g (66%) of magnetic fraction was obtained with 186.23 g of non-magnetic fraction and a loss of 4.81 g (0.86%) reduction in weight to the roasting process at total 150 minutes duration. Roasting temperature ranges between 750^{o}C to 950^{o}C. For the 30 mins roasting presented in figure 4.6, there are four sets of three bars. Each set of three bars represent different roasting circumstance at different temperatures. The first set of bar represents

roasting at 750 ^{o}C and the second set of bars represented 850^{o}C and the last set corresponds with 950^{o}C. The cause of the reduction in weight can be attributed to mass loss of LOI.

Reduction in weight for mixed roasted ore sample was observed in the different rounds of roasting at different temperature and different time. It can be seen from the results that at temperature of 950^{o}C, both roasting time experienced higher reduction in weight of product than 750^{o}C and 850^{o}C. Also, it follows that a total weight of 561.5 g of mixed roasted at temperature range between 750^{o}C to 950^{o}C for 30 minutes, a 1.61g which is 0.29% reduction in weight is expected to affect the weight of the roasted product. Furthermore, for an average weight of 54.7g of mixed ore roasted at temperature range of 750^{o}C to 850^{o}C for 50 minutes, a 4.81g which is 0.86% reduction in weight is expected to affect the weight of the roasted product. Therefore, longer roasting time has higher weight reduction effects than shorter roasting time.

4.7. Phase transformation

A complete magnetite phase was obtained for the sample after roasting at 950 ^{o}C with 10 g of carbon for both 30 and 50 minutes. As shown in the XRD patterns in *figure 4.8 a*, the magnetic fraction of the roasted ore sample at 950^{o}C for 30 to 50 minutes, the quartz , alumina, and some volatile phases of the ore could no longer be seen in the phases present.

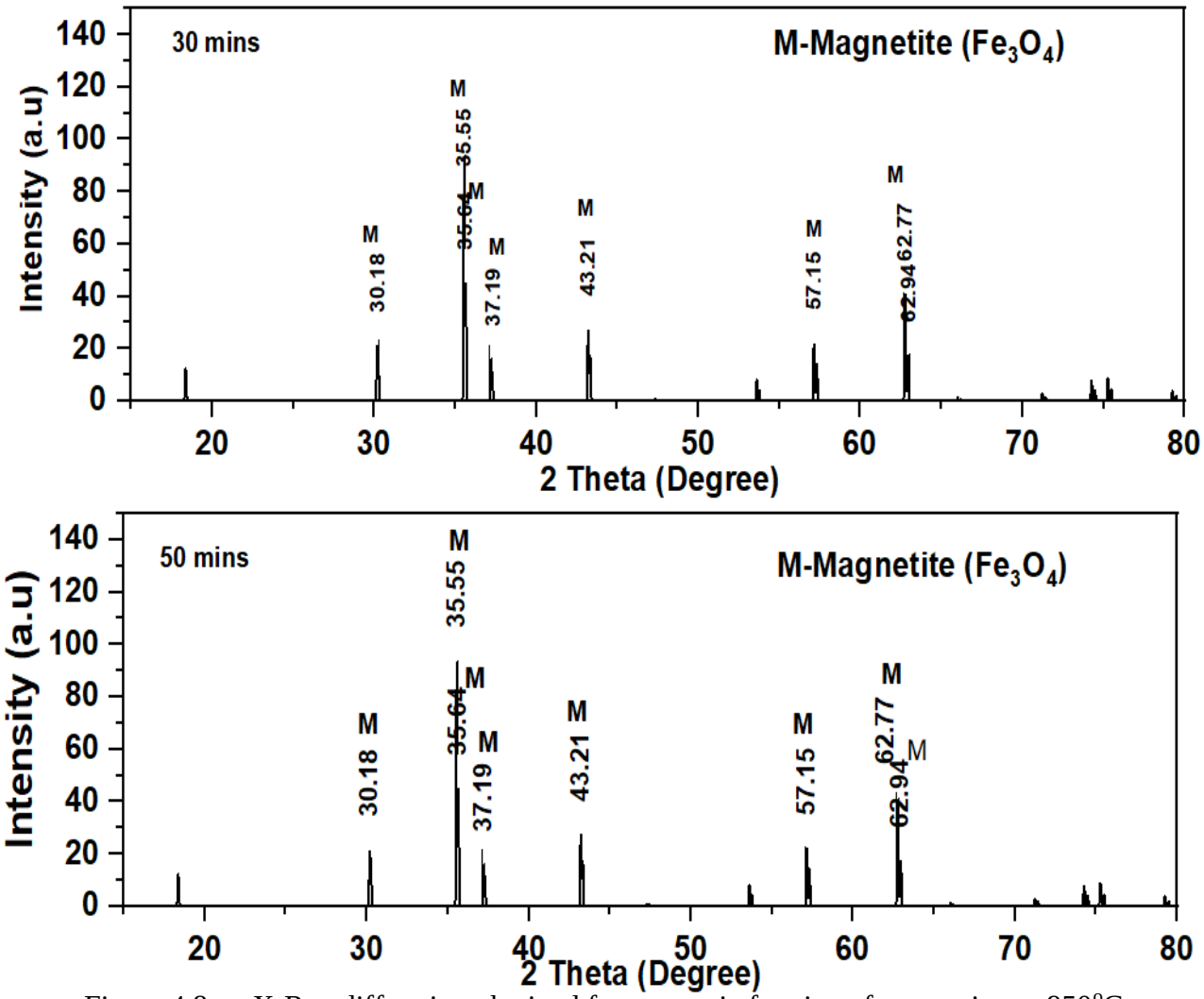

Figure 4.8: a. X-Ray diffraction obtained for magnetic fraction after roasting at 950^{o}C

The major mineral phase that is present is the magnetite phase. Even though there are traces of other minerals present in the ore after roasting, their percentage is very minimal whereas the percentage of the magnetite is approximately 99.9%. This indicates that reduction roasting can be effective in transforming a paramagnetic iron phase to a ferromagnetic iron phase.

A complete magnetite phase is obtained for the sample after roasting at 950 ^{o}C with the amount of carbon for both 30 and 50 minutes. As shown in the XRD patterns in figure 4.8 a, the magnetic fraction of the roasted ore sample after roasting the sample in the furnace at 950^{o}C for

30 to 50 minutes, the quartz , alumina, Cl and Phosphorus and other LOI phases of the ore could

no longer be seen in the phase present. The only mineral phase that is present is the magnetite

phase. Even though there are traces of other elements and compounds present in the ore after roasting, their percentages were very minimal whereas the percentage of the magnetite was approximately 99.9% . This indicates that the reduction roasting can be effective in transforming

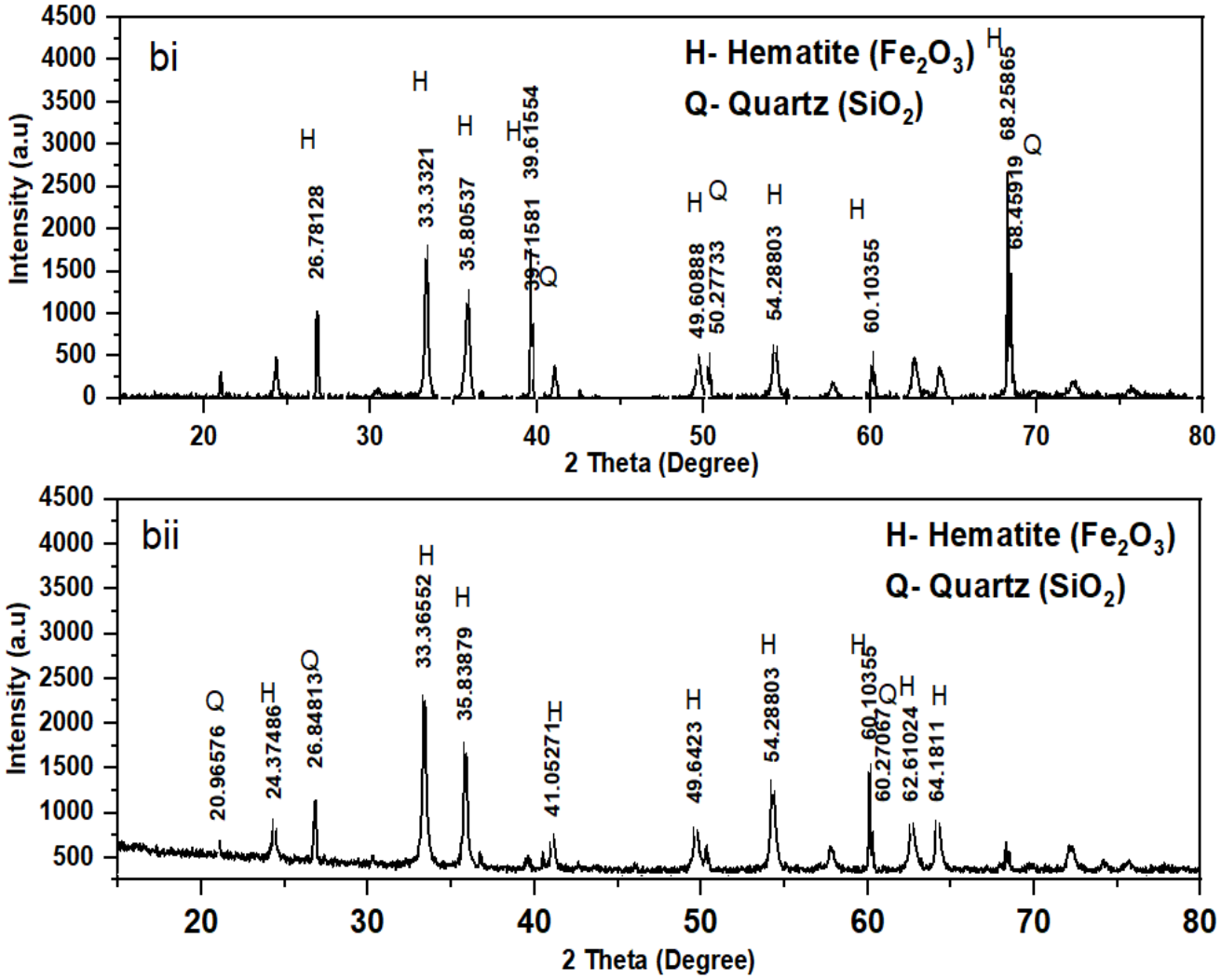

Figure 4.8: b. X-Ray diffraction obtained for magnetic fraction after roasting at 850^{o}C bi: 30 minutes bii: 50 minutes and magnetic separation

a paramagnetic iron phase to a ferromagnetic iron phase. Figure 4.8.b shows dominant hematite mineral phase present in the magnetic fraction after roasting at 850^{o}C for 30 minutes and 50 minutes after magnetic separation. Though hematite and quartz are the phases present in the magnetic fraction of the roasted sample, hematite is predominant than the quartz phase. It is clear from the XRD pattern shown in figure 4.7.b that a complete phase transformation is not obvious for the ore sample at the roasting parameters.

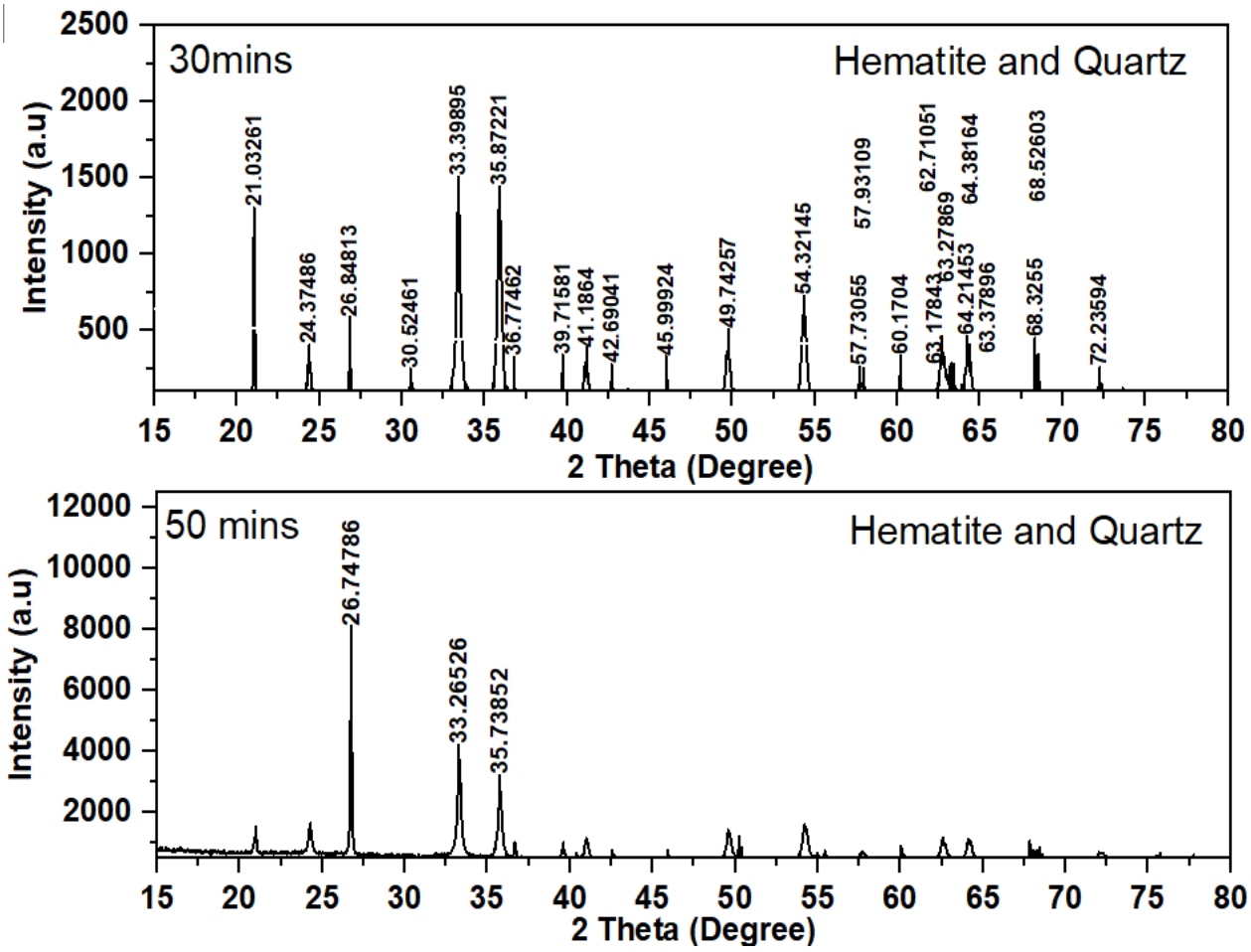

Figure 4.8: c. X-Ray diffraction obtained for magnetic fraction after roasting at 750^{o}C 30 minutes and 50 minutes and magnetic separation

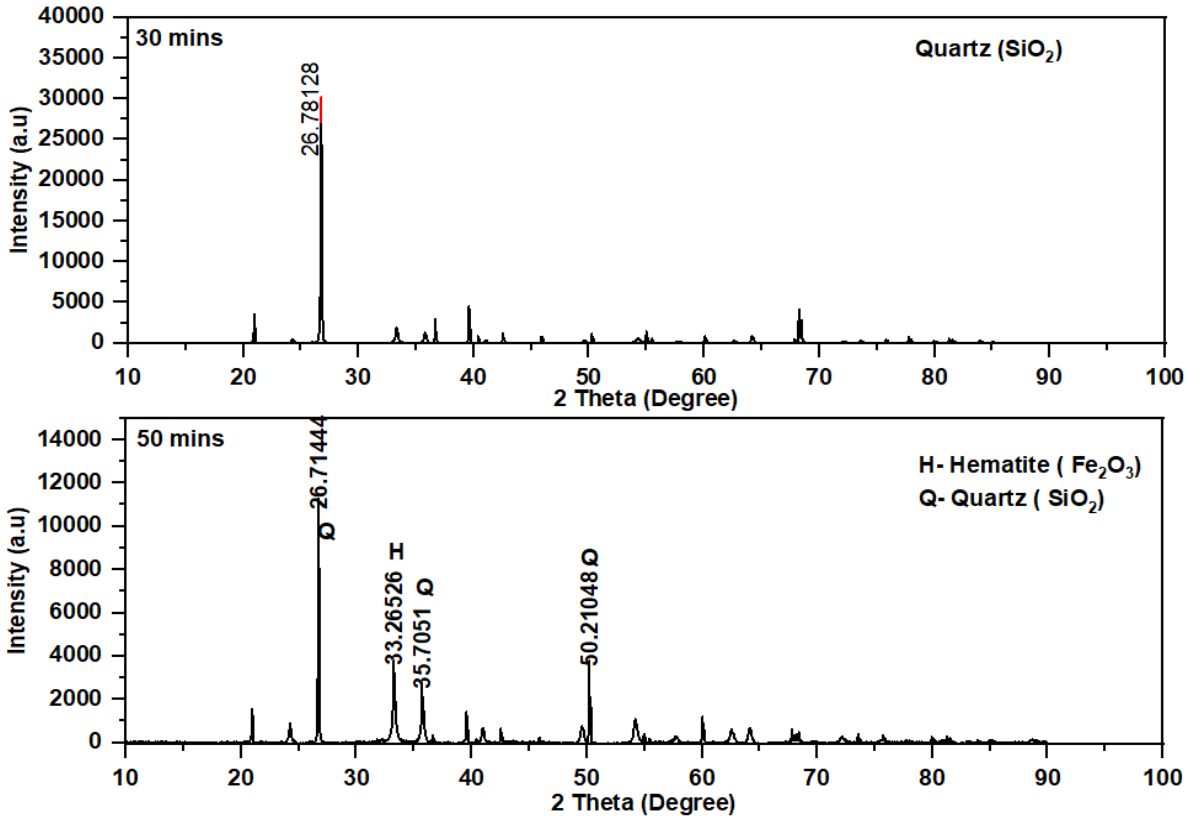

Figure 4.8: d. X-Ray diffraction obtained for non- magnetic fraction after roasting at 750^{o}C and 30 minutes 50 minutes and magnetic separation

As shown in figure 4.8.d,e and f, the quartz and hematite phases as seem to dominate but quartz is more dominant in all roasting conditions than hematite. For the 30 minutes roasting time, quartz was observed to be the dominant phase and for the 50 minutes roasting, quartz was also observed to be the dominant phases present in the sample. Quartz is dominant in the non-magnetic fraction of the roasted sample since it cannot become altered at the temperature ranges mentioned. As seen in the various xrd patterns of the roasted products, complete phase transformation of hematite to magnetite occurred at temperature of 950^{o}C. Below these temperature ranges, complete phase transformation of hematite to magnetite was not observed at temperature between 750^{o}C to 950^{o}C. This is evident in the XRD pattern shown in figure 4.8s.

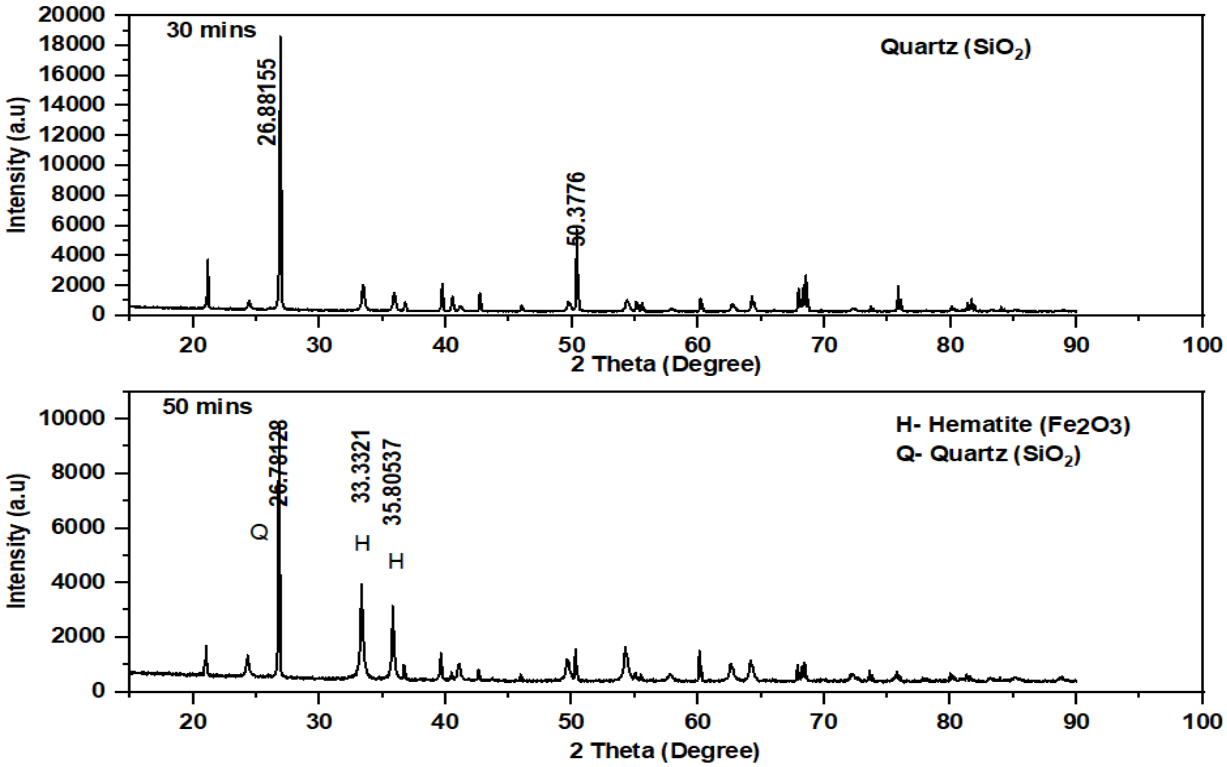

Figure 4.8: e. X-Ray diffraction for non-magnetic fraction after roasting at 850°C minutes and magnetic separation

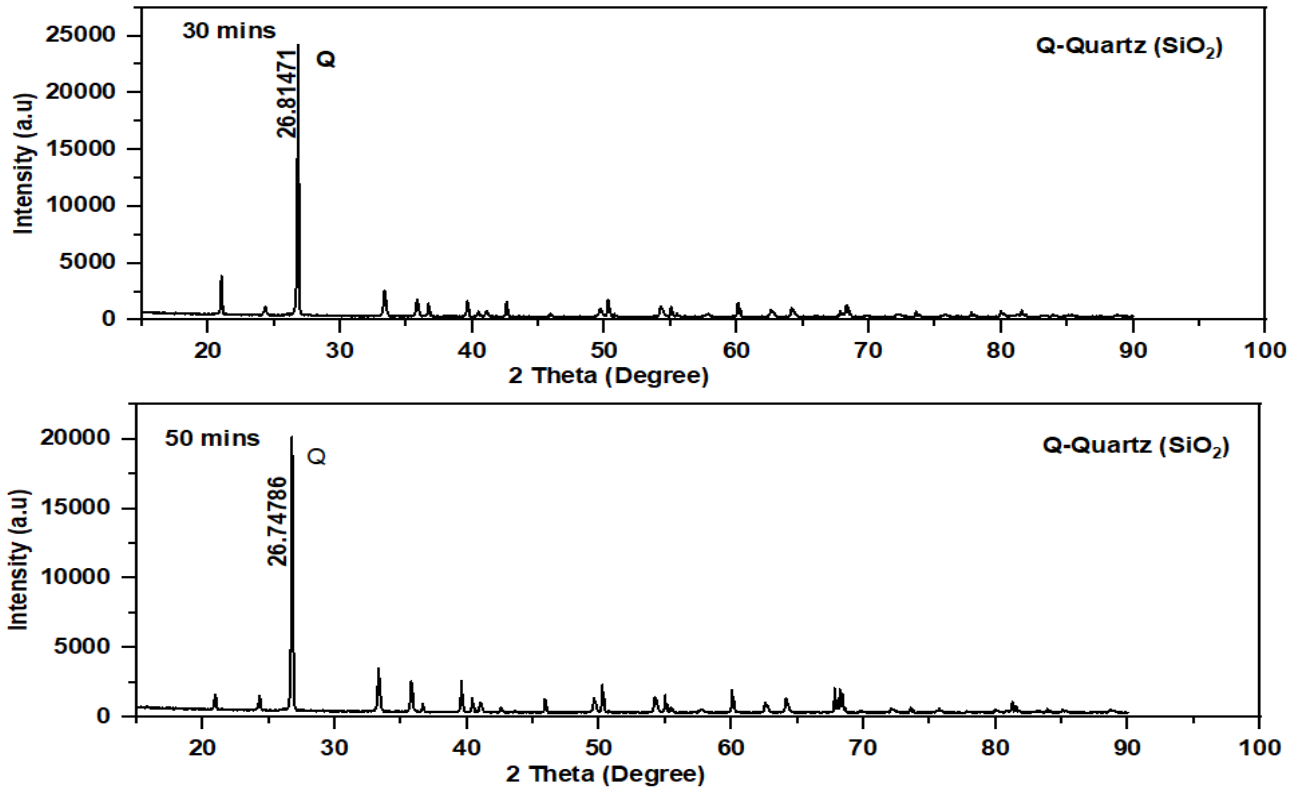

Figure 4.8: f. X-Ray diffraction for non-magnetic fraction after roasting at 750°C minutes and magnetic separation

4.8. Beneficiation study of magnetic technique

As-received material of mass 1684.5 g was crushed, ground, screened and sizes below 2 mm was selected for the study. The weight was chosen in line with the stoichiometry equations presented in Equation 1,2 & 3. 561.5 g of the ore sample was subjected to low intensity dry magnetic separation and 50 g of magnetic fraction was obtained. Following that, the remaining 1123 g of raw ore sample was evenly divided into two fractions and each subjected to three different rounds of reduction roasting for different times and temperature followed by low intensity dry magnetic separation respectively with magnetic intensity of 2000 gauss. 344.86 g of magnetic fraction was obtained from the roasted product followed by separation at magnetic field strength of 2000 gauss for roasting time of 30 minutes at 950oC. 370.46 g of magnetic fraction was obtained from the roasted product followed by separation at magnetic field strength of 2000 gauss for roasting time of 50 minutes at 950^{o}C.

As shown in Table 4.8.a and 4.8.b, reduction in weights of roasted products was observed for each mass of feed that was roasted. The percent reduction in weight varies for all temperatures and all times of roasting. However, the results show that individual weight of magnetic fractions were lower for all temperature ranges than weight of non-magnetic fraction for all round of roasting for 30 minutes, but the total weight of magnetic fraction was greater than the total weight of non-magnetic fraction for the 30 minutes round of roasting. This can be attributed to

Table: 4.8.a: Metallurgical balance for 30 mins roasting

Temperature (^{o}C)	**Weight of Feed (g)**	**Weight of roast (g)**	**Wt of magnetic fraction (g)**	**Wt of Non- magnetic fraction (g)**	**Weight reduction (g)**
750	170.8	170.49	77.76	92.73	0.31
850	194.3	193.76	92.8	100.96	0.54
950	196.4	195.64	174.3	21.34	0.76
	561.5	**559.89**	**344.86**	**215.03**	**1.61**

the presence of deleterious substance in the ore.

Because of the paramagnetic nature of hematite, the unroasted ore responded poorly to magnetism during the first magnetic separation on the raw ore. Also, the presence of hematite in the different phases during the 30 minutes roasted products, the samples responded much better to magnetism than the raw ore sample. As shown in Table 4.7.b, for the 50 minutes roasting, the weight of the magnetic fractions for each round of roasting was greater than the weight the non-magnetic fraction. Consequently, the total weight of the magnetic fraction was approximately two times higher than the total weight of the non-magnetic fractions for the 50 minutes roasting.

Table: 4.8.b: Metallurgical balance for 50 minutes roasting

Temperature (^{o}C)	**Weight of Feed (g)**	**Weight of roast (g)**	**Wt of magnetic fraction (g)**	**Wt of Non- magnetic fraction (g)**	**Weight reduction (g)**
750	170.8	170.35	82.32	88.03	0.45
850	194.3	193.37	112.69	80.68	0.93
950	196.4	194.5	175.45	19.05	1.9
	561.5	**558.22**	**370.46**	**187.76**	**3.28**

4.9. Reduction roasting and Phase compositions

As shown in Table 4.9 a and b, there were great differences in the elemental compositions of the unroasted ore sample and the sample roasted at 950^{o}C for 50mins. The elemental mass of silicon in the as-received ore was 11.866 g but after roasting at 950^{o}C for 50 mins, the elemental mass of silicon in the roasted product was reduced to 6.017 g. The elemental mass of iron improved from 44% in raw ore to 63.2 % in roasted ore sample while the elemental mass of alumina and chlorine remain unchanged.

The elemental mass of oxygen reduces from 37.359 % in raw ore to 24.87 % in roasted ore sample.

Table 4.9: Elemental analysis of as received and roasted at 950^oC

Elements	**As-received Mass (%)**	**Roasted Mass (%)**
Oxygen	37.359	6.017
Aluminum	4.828	4.803
Silicon	11.866	1.77
Chlorine	0.669	0.6
Iron	44.136	86.3
Others	1.142	0.51
	100	100

4.9.1. Reactions involved in the low-grade iron ore reduction.

Several reactions are involved in the complete reduction of hematite to magnetite. These reactions were used to determine the theoretical amounts of carbon required to carry out the reduction process at the various temperatures. Considering that the ore contains Fe_2O_3, Al_2O_3, SiO_2, Cl, P_2O_5, and volatile matter the following reactions presented in equation 1 to 4 were used to determine the theoretical amount of carbon.

$$6Fe_2O_3 + C \rightarrow 4Fe_3O_4 + CO_2 \text{ ……………………… (1)}$$

For the hematite reaction with carbon, 6:1 is the mole ratio and for the balance chemical reaction for complete reduction, 12 gram of carbon is required for 958.14 grams of hematite or 1 tons of hematite would be required for 0.012524 ton of carbon assuming that the ore is pure hematite (1 gram of carbon required for 80 grams of Fe_2O_3).

$$Al_2O_3 + \frac{3}{2}C \rightarrow 2\ Al + + \frac{3}{2}CO_2 \text{...(2)}$$

For complete reduction 1.5 moles of carbon is required for 1mole of Al_2O_3 or 18 grams of carbon is required for 102 grams of Al_2O_3 (1gram of carbon required for 7 grams of Al_2O_3).

$$SiO_2 + C \rightarrow Si + CO_2 \ldots\ldots\ldots\ldots\ldots\ldots\ldots\ldots\ldots\ldots (3)$$

For complete reduction of SiO_2 , 1 mole of carbon is required for 1moles of SiO_2 or 12grams of C for 140 grams of SiO_2 (1 gram of C for 12 grams of SiO_2).

$$P_2O_5 + \frac{5}{2}C \rightarrow 2\,P + \frac{5}{2}CO_2 \ldots\ldots\ldots\ldots\ldots\ldots\ldots\ldots\ldots\ldots\ldots\ldots\ldots\ldots\ldots\ldots\ldots\ldots (4)$$

For complete reduction considering that the material is pure , 2.5 moles of carbon will be required for 1moles of P_2O_5 or 30 grams of carbon for 142 grams of P_2O_5 (1gram of C for 5grams of P_2O_5).

4.9.2 Effect of roasting parameter on iron content

As shown in Table 4.10, reduction roasting had positive impact on the grade and recovery of the magnetic fractions. Because magnetite phase was obtained at 950^{o}C for booth roasting time, the iron content of these two roast products was chosen to tabulate the various effects of various reduction and roasting variables. For the same reductant dosage, particle sizes and temperatures, iron grade changes in the three samples. For the raw ore sample, the iron grade was 63.102 % and 71.2 for the 30 minutes roasting. The iron grade increased from 71.2 % to 86.3 % after 50 minutes roasting at 950^{o}C. The silica content also reduced from 25.381 in the raw sample to 17.36 % in the 30 minutes roasted sample and reduced further down to 4.50% in the magnetic fraction.

Table : 4.10 Effect of roasting parameter on iron content*

Sample	Roasting Time	Temperature	RD	GT	IC [% mass]	SiO_2 Content	Particle Size	Al_2O_3 content
Unroasted	0 mins	25^{o}C	-	2 mins	63.102	25.38	< 2mm	9.11
Roast 1	30 mins	950 ^{o}C	0.02g	2mins	71.2	17.36	< 2mm	9.11
Roast 2	50 mins	950 ^{o}C	0.02g	2 mins	86.3	4.50	< 2mm	9.11

Note: RD : Reductant Dosage; GT : Grinding time; IC: Iron content

4.10. Feasibility of industrial application

Reduction roasting follow by magnetic separation can be a practical way to improve the iron content in a low-grade iron ore. Though suspension roasting and magnetization roasting have not been applied on an industrial skill yet, but the process seems to be practical, but the major cost center will be the energy input during magnetizing roasting. A set up on a pilot scale will further justify their cost. The technique is characterized by short flow processes followed by reduced energy consumption thus has better prospect for industrialization.

5.0. CONCLUSIONS AND RECOMMENDATIONS

5.1. Conclusions

Reduction roasting followed by magnetic separation is a practical beneficiation method for upgrading low-grade iron ore. Roasting parameters for reduction roasting are as follows: 950^{o}C heating temperature, average roasting time of 40 minutes, crushing, grinding, and mixing time of 2 minutes , reductant dosage of 10 g carbon to 565.1 g of sample or 0.02 g carbon to 1-gram ore, and magnetic field strength of 0.2 Tesla. A complete hematite to magnetite phase transformations can be achieved at 950^{o}C for the roasting conditions at or above 30 minutes roasting time. The weight of the magnetic fraction after magnetic separation increased from 344.86 g (61.0%) for 30 minutes roasting to 370.46 g (65.6%) for 50 minutes roasted product followed by magnetic separation. The iron content in the magnetic fraction can be upgraded from 63.1 % to 86.3 % while the silicon content can be reduced from 11.9% to 6.0 %. Increases in roasting time and temperature increased the weight of the magnetic fraction. Carbonized sawdust can serve as a potential source of carbon for use as a reductant. Carbonization of sawdust contributes to waste processing and help save the environment.

5.2 Recommendations / Area of further research

It is recommended that other carbon containing waste materials be investigated for reduction of iron ore; and economic analysis and application of reducing roasting and magnetic separation of low-grade iron be considered.

References

1. A.G. Gunna; J.K. Dorborb; J.M. Mankelowa; P.A.J. Lustya; E.A. Deadyc; R.A. Shawa, K.M. Goodenoughc.(2015). A review of the mineral potential of Liberia. *Ore Geology Review*, pp 413-431
2. Abraham J. B. Muwanguzi, Andrey V. Karasev, Joseph K. Byaruhanga, and Par G. Jonsson (2012), Characterization of the Physical and Metallurgical Properties of Natural Iron Ore for Iron Production. International Scholarly Research Network , ISRN Materials Science; Volume 2012, Article ID 174803, 9 pages .
3. Allen, T. (1997) Particle Size Measurement, Surface Area and Pore Size Determination. 5th Edition, Chapman and Hall, New York, 149.
4. Anon (1988). Test sieving , British Standard 1796-1: 1989, ISO 2591-1: 1988.
5. Anon. (2000). Methods using test sieves of woven wire cloth and perforated metal plate. British Standard 410-1: 2000, ISO 3310- 1: 2000. Test sieves. *Technical requirements and testing.*
6. Benchiheub O, Mechachti S, Serrai S, Khalifa MG. (2010). Elaboration of iron powder from mill scale. Mater. Environ. Sci. 1 (4) (2010) 267-276 J
7. Burt, R.O. (1985). Gravity Concentration Technology, *Elsevier, Amsterdam*.
8. C.L.Luke (1968). Determination of trace elements in inorganic and organic materials by x-ray fluorescence spectroscopy. Analytica Chimica Acta Volume 41, 1968, Pages 237-250
9. Christopher. P. Brough, Petrolab Limited, James Strongman, Petrolab Limited, John Fletcher, Mariola Zając Operational mineralogy: an overview of key practices in

sample analysis, sample preparation and statistics August 2019 Conference: 15th SGA Biennial Meeting 2019 At: University of Glasgow

10. Claus Bernhardt (1994); Particle Size Analysis: Classification and sedimentation methods. Technical University of Mining Academy Freiberg, Germany
11. Daniel Spreitzer and Johannes Schenk (2019); Reduction of Iron Oxides with Hydrogen—A Review. Steel Research International , Volume 90 Issue 10
12. Das, S. K.; Das, B.; Saktivel, R.; Mishra, B. K. (2010). Mineralogy, microstructure, and chemical composition of goethites in some iron ore deposits of Orissa, India. *Miner. Process. Extract. Metall*. Rev., 31: 97–110
13. Donskoi, E.; Collings, A. F.; Poliakov, A.; Bruckard, W. J. (2012) Utilization of ultrasonic treatment for upgrading of hematitic/goethitic iron ore fines. Int. J. Miner. Process., 114–117:80–92
14. Dudchenko, N.O., Ponomar, V.P., 2015. Phase transformation of goethite into magnetite by reducing with carbohydrates. Dnipropetr. Univ. Bull. Ser.: Geol., Geogr. 23 (1), 24–32.
15. Erick R. Force (1983). Geology of Nimba County, Liberia. Received from: I. Liberian Geological Survey. II. United States. Agency for International Development. III. Title. IV. Series
16. Fatbi Habashi. (1997). Handbook of Extractive Metallurgy: The Beginnings of Mining and Metallurgical Education; Volume 2 160 pages, ISBN 2-922686-12-4
17. Gaviria, J.P., Bohe, A., Pasquevich, A., Pasquevich, D.M. (2007). Hematite to magnetite reduction monitored by Mossbauer spectroscopy and X-ray diffraction. *Physica B 389*, 198–201

18. Gaviria, J.P., Bohe, A., Pasquevich, A., Pasquevich, D.M., 2007. Hematite to magnetite reduction monitored by Mossbauer spectroscopy and X-ray diffraction. Physica B 389, 198–201.
19. Grace Ofori-Sarpong, Charles Ebenezer Abbey, Richmond Komla Asamoah, Richard Kwasi Amankwah.(2014). Bauxite Enrichment by Microwave-Magnetizing Roasting Using Sawdust as Reducing Agent. *American Journal of Chemical Engineering. Vol. 2*, pp. 59-64.
20. H. İbrahim Ünal , Enes Turgut , Ş. H. Atapek, Attila Alka. (2015). Direct Reduction of Ferrous Oxides to form an Iron-Rich Alternative Charge Material; High Temp. Mater. Proc. 2015; 34(8): 751–756
21. Iron Ore Mineral (2014). Received from Arcelor Mittal University
22. J. Bessières, A. Bessières, J.J. Heizmann. (1980). Iron oxide reduction kinetics by hydrogen. International Journal of Hydrogen Energy, Volume 5, Issue 6, 1980, pp. 585-595.
23. Jiang, T., Liu, M.D., Li, G., Sun, N., Zeng, J.H., Qiu, G.Z., (2010). Novel process for treatment of high-aluminum limonite ore by reduction roasting with addition of sodium salts. *Chin. J. Nonferrous Metals* 20, 565e571.
24. John W. Berge (1966). The geology and origin of the Precambrian Goe Range iron formation and associated metasediments; Geological Forefinger I Stockholm Rehandling Volume 95, 1973 - Issue 4, Taylor and Francis Online
25. Lev S. Zevin and Giora Kimmel (1995). Quantitative X-Ray Diffractometry, Springer

26. M. Kumar, S. Jena, and S. K. Patel. (2008). Characterization of properties and reduction behavior of iron ores for application in sponge ironmaking. *Mineral Processing and Extractive Metallurgy Review*, vol. 29, no. 2, pp. 118–129,
27. Man Kee Lam, Ridzuan Zakaria (2008). Production of activated carbon from sawdust using fluidized bed reactor; International Conference on Environment (ICENV 2008).
28. Mazurov EF, Gnuchev SM, Skripchuk VS, Markin AA, Lyalin ES. (2015). Metallurgist, High Temperature Materials and Process, Volume 34 Issue 8
29. Michael C. Meyer Peter Austin Peter Tropper (2013) Quantitative evaluation of mineral grains using automated SEM–EDS analysis and its application potential in optically stimulated luminescence dating. Radiation Measurements Volume 58, , Pages 1-11
30. Mishra, B. K.; Reddy, P. S. R.; Das, B.; Biswal, S. K.; Prakash, S.; Das, S. K. (2007) Issues relating to characterization and beneficiation of low-grade iron ore fines. *Steel World*, 11–12, 34–36
31. Mishra, B. K.; Reddy, P. S. R.; Das, B.; Biswal, S. K.; Prakash, S.; Das, S. K. (2007). Issues relating to characterization and beneficiation of low-grade iron ore fines. *Steel World*, 11–12, 34–36
32. Nuspl, M., Wegscheider, W., Angeli, J. *et al (2004).* Qualitative and quantitative determination of micro-inclusions by automated SEM/EDX analysis. *Anal Bioanal Chem* **379,** 640–645
33. P Somasundaram, Thomas W Healy, DW Fuerstenau (1964). Surfactant adsorption at the solid—liquid interface—dependence of mechanism on chain length.The Journal

of Physical Chemistry Volume 68 Issue12 Pages 3562-3566 Publisher American Chemical Society

34. P. Somasundaram and D. W. Fuerstenau (1966). Mechanisms of Alkyl Sulfonate Adsorption at the Alumina-Water Interface1; The Journal of Physical Chemistry 70 (1), 90-96
35. Paul J. Sylvester (2019). The Application of Automated SEM-Based Identification of Detrital, Diagenetic and Indicator Mineral Phases . Minerals Special Issues
36. Rao et al(2013) . Trace elemental analysis of Indian natural moonstone gems by PIXE and XRD technique. Appl. Radiat. Isot. 82 211–222
37. Rolf Fandrich Ying Gu Debra Burrows Kurt Moeller (2007), Modern SEM-based mineral liberation analysis, International Journal of Mineral Processing Volume 84, Issues 1–4, 19, Pages 310-320
38. S. S. Rath, H. Sahoo,N. Dhawan,D. S. Rao,B. Das &B. K. Mishra (2014). Optimal Recovery of Iron Values from a Low-Grade Iron Ore using Reduction Roasting and Magnetic Separation. Separation Science and Technology, Volume 49- 2014 Issue 12
39. Stephen Wagner., Daniela Sauer.,Christine Stein,. Karl Stahr (2006). Soil development on a flight of marine terraces in Metaponto, Southern Italy - WCSS Philadelphia
40. Sun, Jie; Zhang, Jin Zhu (2013). Beneficiation Study on an Oolitic Hematite. Advanced Materials Research, 690-693(), 202–205.
41. Svoboda, J. (1987) Magnetic methods for treatment of minerals . In: Developments in Mineral processing; *M*agnetic Separation News.Voi.2,pp.223-224

42. The Southern African Institute of Mining and Metallurgy (2009). Evaluation of iron ore pellets and sinters for BF and DR use. Received from: http://www.saimm.co.za/events/0809pelsint/downloads/Mashao.pdf.
43. Tülay TÜRK, Sultan GÖÇER, M. Kadir GÜNER , Burakhan ERSOY , Enes KALYONCU , Gülay BULUT (2019). Developments in Flotation Technology, IMPC Eurasia Conference
44. U.S. Geological Survey. Mineral commodity summaries 2012. Reston: The U.S. Government Printing Office; 2012.
45. Yongshi Jin, Tao Jiang, Yongbin Yang, et al: Central. South. University. Technology. Vol. 6 (2006), P. 673
46. Zhang, M., Hui, Q., Lou, X.-J., Redfern, S.A.T., Salje, E.K.H. & Tarantino, S. (2006) Dehydroxylation, proton migration, and structural changes in heated talc: an infrared spectroscopic study. American Mineralogist, 91, 816–825